An Illustrated Key to the Mandibles of Small Mammals of Eastern Canada

Dominique Fauteux[1, 4], Gilles Lupien[2], François Fabianek[3], Jonathan Gagnon[1], Marion Séguy[1], Louis Imbeau[1]

[1]Chaire industrielle CRSNG-UQAT-UQAM* en aménagement forestier durable and Centre d'étude de la forêt, Université du Québec en Abitibi-Témiscamingue, Rouyn-Noranda, Québec J9X 5E4 Canada
[2]Ministère du Développement durable, de l'Environnement, de la Faune et des Parcs, Direction régionale du Saguenay-Lac Saint-Jean, Jonquière, Québec G7X 8L6 Canada
[3]Centre d'étude de la forêt, Faculté de foresterie, géographie et géomatique, Université Laval, Québec, Québec G1V 0A6 Canada
[4]Corresponding author: dominique.fauteux.1@ulaval.ca

Fauteux, Dominique, Gilles Lupien, François Fabianek, Jonathan Gagnon, Marion Séguy, and Louis Imbeau. 2014. An illustrated key to the mandibles of small mammals of eastern Canada. Canadian Field-Naturalist 128(1): 25–37.

Skulls are often used to identify small mammals, and most identification keys to small mammals have been developed on the assumption that whole skulls will be available. However, the skulls of small mammals are seldom found intact in predator pellets or nests, and the bones of several individuals are often scattered and mixed, making counting impossible without the use of a specific cranial part. In addition, only a few keys include all the species found in the eastern provinces of Canada.

Mandibles readily resist degradation by the gastric acids of both avian and mammalian predators and are often found intact in food caches of mustelids and in bat hibernacula. We therefore designed an illustrated dichotomous key to small mammals (mean mass <5 kg) of eastern Canada based on diagnostic mandible characters (including the teeth and one dentary bone). We identified and confirmed diagnostic characters to distinguish 55 species from the orders Lagomorpha, Rodentia, Soricomorpha, Carnivora, and Chiroptera. These diagnostic characters are based on a review of the literature and were confirmed by measurements performed on both museum and trapped specimens. In order to facilitate identification, photographic illustrations are provided for each couplet of the key.

The ability to identify small mammals using their mandibles will reduce the number of skull components needed and has proven to be a useful tool in the study of the diet of predators. This key may also be helpful in identifying bats in the genera *Myotis*, *Perimyotis*, and *Eptesicus*, which are presently affected by the spread of white-nose syndrome (caused by *Pseudogymnoascus destructans*) throughout the eastern part of Canada.

Key Words: Lagomorpha; Rodentia; Soricomorpha; Carnivora; Chiroptera; shrews; moles; voles; lemmings; mice; bats; hares; weasels; lower jaw; skull; dentary; eastern Canada

Introduction

Small mammals consumed by predators are particularly difficult to identify because their skulls are often physically damaged or they have been degraded by gastric acids (Mayhew 1977). Cranial bones that resist degradation often disassociate from the larger component they were affixed to and are often found scattered in predator scats, pellets, or nests (Buidin *et al.* 2007; Khalafalla and Iudica 2010). They may also be found as concentrations of loose bones near caves or other shelters used by predators (Buden 1974). Predators such as mustelids have "food caches" in which they store carcasses for later consumption (Oksanen *et al.* 1985). As a result, prey remains may be disassociated and may accumulate.

Several published keys to small mammal skulls are based on the assumption that the whole skull is available (van Zyll de Jong 1983; Glass and Thies 1997; Lupien 2001, 2002; Nagorsen 2002; Chapman *et al.* 2007), but this is rarely the case with prey remains (Mollhagen *et al.* 1972; Buden 1974; Balciauskiene *et al.* 2002). Furthermore, loose bones of different individual prey items are often mixed. The minimum number of individuals is a derived unit of abundance often used in paleozoology (Lyman 2008). By using a single skull component, this method avoids overestimating species abundance in bone aggregations. The mandible has been proposed as a useful cranial component for identifying groups of mammals (Roest 1991; Balciauskiene *et al.* 2002), but it has rarely been used to identify mammals to the species level, except for shrews (Repenning 1967; Carraway 1995).

The mandible, or lower jaw, is composed of teeth and a pair of dentary bones (Figure 1). The teeth of the mandible are often referred to as the lower dentition, and each tooth is identified with a lower case letter (i.e., p3 for the third premolar). For the present article, we focused on the mandible and thus omitted the term "lower". Because the left and right dentary often separate as a result of degradation, it is imperative that the same dentary bone (i.e., left or right, but not both) be used for counting purposes.

Several diagnostic characters make the mandible an ideal tool for identifying most mammalian species that have very few but sturdy bones. The size, the dental formulae, and the occlusal patterns of the molar enamel are key characteristics that are often used in keys to skulls (Repenning 1967; Glass and Thies 1997; Lupien 2002; Nagorsen 2002). Furthermore, diagnostic characters of the dentary bones are found on both the anterior and the posterior parts. The size and shape of the lower edge of the ramus and the position of the mental and dental foramina, as well as the size and shape of the condylar, coronoid, and angular processes, are useful characters requiring only a few metric measurements (Roest 1991; Carraway 1995).

We present an identification key to the mandibles of all established small mammals (mean mass of <5 kg) of eastern Canada to assist in the identification of prey remains and other types of loose bones when skulls are incomplete or damaged. Each criterion mentioned in the couplets of the key is illustrated by a picture as a visual support. A glossary and the general nomenclature are also provided.

Methods

According to Merritt (2010), mammals may be categorized as small when the average mass of the species is less than 5 kg. Based on this criterion, we selected all the small mammals established in the provinces of Ontario, Quebec, Newfoundland and Labrador, Prince Edward Island, New Brunswick, and Nova Scotia (Peterson 1966; Banfield 1974; Dobbyn 1994; Desrosiers *et al.* 2002; Naughton 2012). The general taxonomy used in the key is listed in Table 1.

This key summarizes all diagnostic mandible characters that we have found in the literature for the orders Lagomorpha (Roest 1991), Rodentia (Klingener 1963; Phillips and Oxberry 1972; Grayson *et al.* 1990; Roest 1991; Lupien 2002; Chapman *et al.* 2007), Soricomorpha (Hallet 1978; Yates and Schmidly 1978; van Zyll de Jong 1983; Carraway 1995; Glass and Thies 1997; Lupien 2001), Carnivora (Roest 1991; Glass and Thies 1997), and Chiroptera (Gaudin *et al.* 2011). Certain species were very difficult to distinguish using the morphologic features of the mandible alone. Therefore, we included morphometric measurements such as the length of the mandible, the length of the mandibular tooth row, and the height of the coronoid process when two species or groups of species could be distinguished only by size.

We validated the mandible characteristics presented in this key by studying specimens from Ontario, Quebec, Newfoundland and Labrador, Prince Edward Island, New Brunswick, and Nova Scotia preserved in the Canadian Museum of Nature and Université Laval. Morphometric measurements were validated on 10 specimens of each species when possible. Otherwise, all specimens available were used. We further extracted a sample of reference mandibles from complete frozen specimens, in collaboration with the Ministère du Développement durable, de l'Environnement, de la Faune et des Parcs du Québec and the Université du Québec à Rimouski, and from specimens trapped during a related study (Fauteux *et al.* 2012). The relevance of the diagnostic characters in identifying prey remains was validated by Séguy (2010) using nest remains to quantify the diet of Northern Saw-whet Owls (*Aegolius acadicus*).

Results and Discussion

We found that 55 of the 60 small mammal species of eastern Canada could be identified from their mandibles. The White-footed Mouse (*Peromyscus leucopus*) and the Deer Mouse (*P. maniculatus*) could not be identified to the species level, because their mandibles are identical. Although both *Peromyscus* species may be differentiated using several skull measurements, biochemical and genetic markers are probably the only reliable methods to date (Aquadro and Patton 1980; Rich *et al.* 1996). Similarly, three species of lagomorphs (i.e., *Lepus arcticus*, *L. europaeus*, and *L. townsendii*) could not be distinguished using the mandibles alone.

Consulting species' distribution may facilitate identification of small mammals (Banfield 1974; Desrosiers *et al.* 2002; Naughton 2012). For example, *Sciurus*

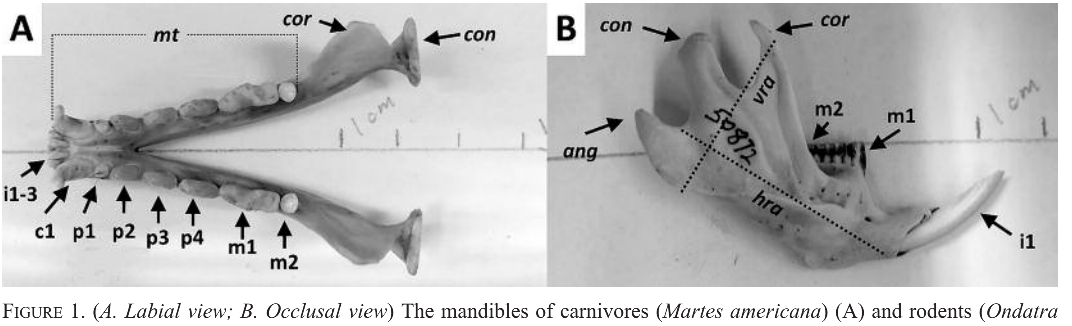

FIGURE 1. (*A. Labial view; B. Occlusal view*) The mandibles of carnivores (*Martes americana*) (A) and rodents (*Ondatra zibethicus*) (B). Labels refer to the incisor (i), canine (c), premolar (p), molar (m), mandibular tooth row (*mt*), coronoid process (*cor*), condyle (*con*), angular process (*ang*), vertical ramus (*vra*), and horizontal ramus (*hra*).

TABLE 1. Common and scientific names of the small mammals <5 kg in eastern Canada identified in the dichotomous key (Peterson 1966; Banfield 1974; Wilson and Reeder 2005; Hoofer *et al.* 2006; Naughton 2012; ITIS 2013).

Order	Family	Scientific name	Common name (English)	Nom commun (français)
Rodentia	Cricetidae	*Dicrostonyx hudsonius*	Ungava Collared Lemming	Lemming d'Ungava
		Microtus chrotorrhinus	Rock Vole	Campagnol des rochers
		Microtus pennsylvanicus	Meadow Vole	Campagnol des champs
		Microtus pinetorum	Woodland Vole	Campagnol sylvestre
		Myodes gapperi	Southern red-backed Vole	Campagnol à dos roux de Gapper
		Myodes glareolus	Bank Vole	Campagnol roussâtre
		Ondatra zibethicus	Common Muskrat	Rat-musqué commun
		Peromyscus leucopus	White-footed Mouse	Souris à pattes blanches
		Peromyscus maniculatus	Deer Mouse	Souris sylvestre
		Phenacomys ungava	Eastern Heather Vole	Phénacomys
		Synaptomys borealis	Northern Bog Lemming	Lemming des tourbières
		Synaptomys cooperi	Southern Bog Lemming	Lemming de Cooper
	Dipodidae	*Napaeozapus insignis*	Woodland Jumping Mouse	Zapode des bois
		Zapus hudsonius	Meadow Jumping Mouse	Zapode des champs
	Erethizontidae	*Erethizon dorsatum*	North American Porcupine	Porc-épic d'Amérique
	Muridae	*Mus musculus*	Common Mouse	Souris commune
		Rattus norvegicus	Norway Rat	Rat surmulot
	Sciuridae	*Glaucomys sabrinus*	Northern Flying Squirrel	Grand polatouche
		Glaucomys volans	Southern Flying Squirrel	Petit polatouche
		Marmota monax	Woodchuck	Marmotte commune
		Poliocitellus franklinii	Franklin's Ground Squirrel	Spermophile de Franklin
		Tamias minimus	Least Chipmunk	Tamia mineur
		Tamias striatus	Eastern Chipmunk	Tamia rayé
		Tamiasciurus hudsonicus	Red Squirrel	Écureuil roux
		Sciurus carolinensis	Eastern Gray Squirrel	Écureuil gris
		Sciurus niger	Eastern Fox Squirrel	Écureuil fauve
Lagomorpha	Leporidae	*Lepus americanus*	Snowshow Hare	Lièvre d'Amérique
		Lepus arcticus	Arctic Hare	Lièvre arctique
		Lepus europaeus	European Hare	Lièvre d'Europe
		Lepus townsendii	White-tailed Jackrabbit	Lièvre de Townsend
		Sylvilagus floridanus	Eastern Cottontail	Lapin à queue blanche
Carnivora	Canidae	*Urocyon cinereoargenteus*	Grey Fox	Renard gris
		Vulpes lagopus	Arctic Fox	Renard arctique
		Vulpes vulpes	Red Fox	Renard roux
	Mephitidae	*Mephitis mephitis*	Striped Skunk	Moufette rayée
	Mustelidae	*Martes americana*	American Marten	Martre d'Amérique
		Martes pennanti	Fisher	Pékan
		Mustela erminea	Ermine	Hermine
		Mustela frenata	Long-tailed Weasel	Belette à longue queue
		Mustela nivalis	Least Weasel	Belette pygmée

TABLE 1. (*continued*) Common and scientific names of the small mammals <5 kg in eastern Canada identified in the dichotomous key (Peterson 1966; Banfield 1974; Wilson and Reeder 2005; Hoofer *et al.* 2006; Naughton 2012; ITIS 2013).

Order	Family	Scientific name	Common name (English)	Nom commun (français)
		Neovison vison	American Mink	Vison d'Amérique
Soricomorpha	Soricidae	*Blarina brevicauda*	Northern Short-tailed Shrew	Grande musaraigne
		Sorex arcticus	Arctic Shrew	Musaraigne arctique
		Sorex cinereus	Cinereous Shrew	Musaraigne cendrée
		Sorex dispar	Long-tailed Shrew	Musaraigne longicaude
		Sorex fumeus	Smoky Shrew	Musaraigne fuligineuse
		Sorex hoyi	North American Pygmy Shrew	Musaraigne pygmée
		Sorex maritimensis	Maritime Shrew	Musaraigne des Maritimes
		Sorex palustris	North American Water Shrew	Musaraigne palustre
	Talpidae	*Condylura cristata*	Star-nosed Mole	Condylure à nez étoilé
		Parascalops breweri	Hairy-tailed Mole	Taupe à queue velue
		Scalopus aquaticus	Eastern Mole	Taupe à queue glabre
Chiroptera	Vespertilionidae	*Eptesicus fuscus*	Big Brown Bat	Grande chauve-souris brune
		Lasionycteris noctivagans	Silver-haired Bat	Chauve-souris argentée
		Lasiurus borealis	Eastern Red Bat	Chauve-souris rousse
		Lasiurus cinereus	Hoary Bat	Chauve-souris cendrée
		Myotis leibii	Eastern Small-footed Myotis	Chauve-souris pygmée
		Myotis lucifugus	Little Brown Myotis	Petite chauve-souris brune
		Myotis septentrionalis	Northern Myotis	Chauve-souris nordique
		Perimyotis subflavus	Tri-colored Bat	Pipistrelle de l'Est

niger are found only in extreme southern Ontario, and the distribution of *Sorex maritimensis* is restricted to New Brunswick and Nova Scotia.

The mandible is highly polymorphic between and within orders. The order Soricomorpha can be distinguished from other orders because the canine is similar in size to the premolars and the angular process is long and slender (Figure 2B) (key section D). In Lagomorpha, the large angular process and the very small coronoid process are probably the most distinctive characters (Figure 3A) (key section B). In contrast, species of the order Rodentia have a well-developed coronoid process, often with complex occlusal patterns on the molars (Figures 3B) (key section C). Carnivores have large canines and a coronoid process that is disproportionately larger than the condyle and the angular process (Figure 4B) (key section E). Species from the order Chiroptera are mainly characterized by the relatively small vertical ramus and the conspicuous bump on the lower edge of the horizontal ramus beneath the canine (Figure 5B) (key section F).

In some cases, mandibles may be broken and/or teeth may be missing. To address this problem, we provide two or more criteria. However, we struggled to find more than one mandibular characteristic in certain groups of species. In the orders Lagomorpha and Carnivora, only the length of the mandibular tooth row and the height of the coronoid process may be used effectively to distinguish the hares (*Lepus* spp.) and the weasels (*Mustela* spp.). Voles and lemmings may be more effectively differentiated with dental criteria, and identifications may become difficult when the teeth are missing (Banfield 1974; Lupien 2002). Although identifications using heavily degraded mandibles (e.g.,

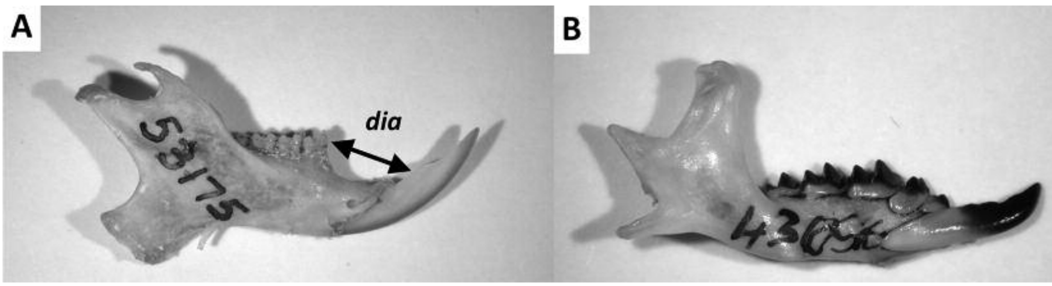

FIGURE 2. (*labial view*) Dentary bone of rodents with a large diastema (*dia*) (*Glaucomys volans*) (A), and soricomorphs (*Blarina brevicauda*) (B).

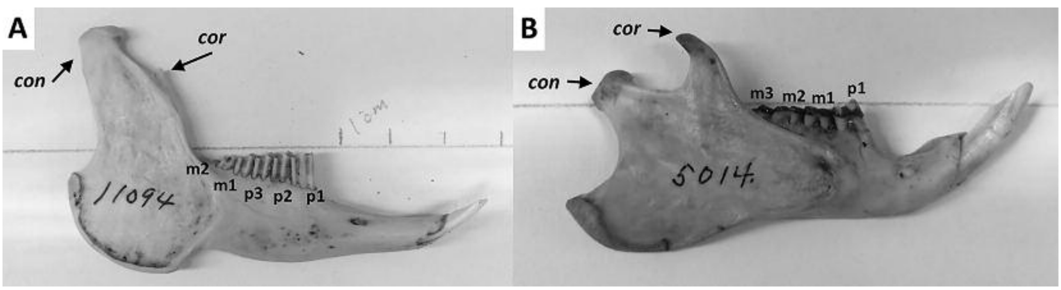

FIGURE 3. (*labial view*) Coronoid process (*cor*) and condyle (*con*) of lagomorphs (*Lepus arcticus*) (A) and rodents (*Marmota monax*) (B).

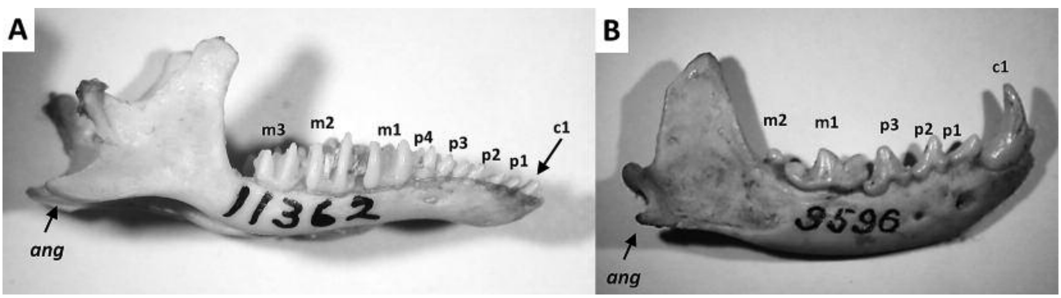

FIGURE 4. (*labial view*) Size of the angular process as well as the size of the canine compared to the adjacent premolar in soricomorphs (*Parascalops breweri*) (A) and carnivores (*Neovison vison*) (B).

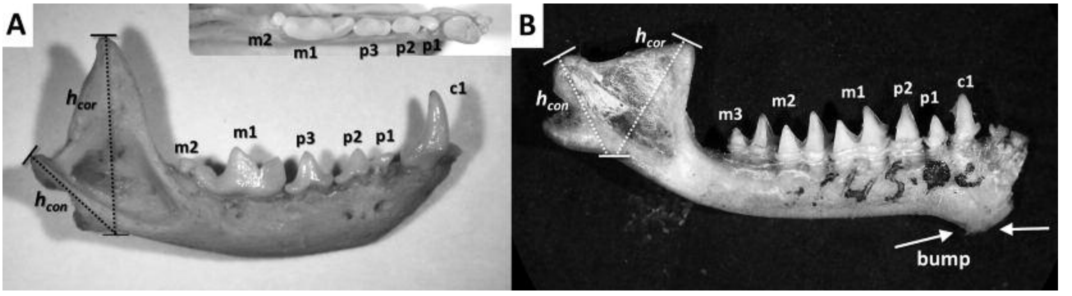

FIGURE 5. (*labial view*) Dentary bones of carnivores (*Mustela erminea*) (A) and chiropterans (*Perimyotis subflavus*) (B) with the height of the condyle (h_{con}), height of the coronoid process (h_{cor}), and the conspicuous mandibular bump of chiropterans.

complete absence of teeth on specimens of Cricetidae) may be generalized, the resistance of mandibles to degradation and the number of criteria we included in the key should prove useful in identifying lightly degraded mandibles to the species level.

Sex and age are important factors that may mean that certain mandible criteria may not be useful (because of sexual dimorphism and growth). We acknowledge that this may be a limitation to a key based on osteometry. Identifications conducted on bones of juveniles that are mixed with bones of adult prey may have a lower resolution (i.e., identifications stop at the genus level) than when only adults are present. As a solution, we included in the vast majority of couplets one or more known morphologic characters that are persistent through age and that do not differ between males and females, such as the morphology of the ramus. Using the mandible is also a useful tool for the counting of individual remains and do not necessitate lengthy and costly methods that often require advanced laboratory skills (e.g., identifications using DNA).

This is a new tool for identifying and monitoring all of the small mammals of eastern Canada. To our knowledge, this is the first comprehensive key designed in North America that uses the mandible exclusively. Use of the mandible enables degraded specimens of most small mammals to be identified down to the species level and it facilitates counting activities. Moreover, bats of the genera *Myotis*, *Perimyotis*, and *Eptesicus* have declined dramatically in the past few years as a result of the spread of white-nose syndrome (caused by *Pseudogymnoascus destructans*) in the eastern part of the United States and Canada (Blehert *et al.* 2009). Identifying mandibles on the floor of caves and in other hibernacula might be useful for monitoring carcasses.

Acknowledgements

Financial support was provided by the Natural Sciences and Engineering Research Council of Canada (NSERC) and the Fonds de recherche du Québec – Nature et technologies (FRQNT) of Quebec. We thank the Centre for Forest Research and the Conseil de recherches en sciences naturelles et en génie du Canada – Université du Québec en Abitibi-Témiscamingue–Université du Québec à Montréal (CRSNG-UQAT-UQAM) Industrial Chair in Sustainable Forest Management for technical support. We thank the Canadian Museum of Nature and Michel Gosselin and Kamal Khidas (both of the Canadian Museum of Nature) for their help with the skull collection and for providing us with a digital camera attached to a binocular. We thank David W. Nagorsen for providing constructive comments on earlier versions of the manuscript. We thank Amélie Drolet for linguistic revision of the text. We also thank all field assistants who participated in the collection of bones and the small mammal trapping campaigns.

Literature Cited

Aquadro, C. F., and **J. C. Patton.** 1980. Salivary amylase variation in *Peromyscus*: use in species identification. Journal of Mammalogy 61: 703–707.

Balciauskiene, L., R. Juskaitis, and **R. Mazeikyte.** 2002. Identification of shrews and rodents from skull remains according to the length of a tooth row. Acta Zoologica Lituanica 12: 353–361.

Banfield, A. W. F. 1974. The mammals of Canada. University of Toronto Press, Toronto, Ontario, for the National Museum of Natural Sciences, National Museums of Canada. 438 pages.

Blehert, D. S., A. C. Hicks, M. Behr, C. U. Meteyer, B. M. Berlowski-Zier, E. L. Buckles, J. T. H. Coleman, S. R. Darling, A. Gargas, R. Niver, J. C. Okoniewski, R. J. Rudd, and **W. B. Stone.** 2009. Bat white-nose syndrome: an emerging fungal pathogen? Science 323: 227.

Buden, D. W. 1974. Prey remains of Barn Owls in the southern Bahama Islands. Wilson Bulletin 86: 336–343.

Buidin, C., Y. Rochepault, and **J. P. L. Savard.** 2007. Régime alimentaire de la Nyctale de Tengmalm en Minganie durant la nidification. Naturaliste canadien 131: 28–33.

Carraway, L. N. 1995. A key to recent Soricidae of western United States and Canada based primarily on dentaries. Museum of Natural History, University of Kansas, Lawrence, Kansas. 48 pages.

Chapman, B. R., S. B. Castleberry, and **J. Laerm.** 2007. Dichotomous keys to the mammals of the South by order. Pages 35–56 *in* The Land Manager's Guide to Mammals of the South. *Edited by* M. K. Trani, W. M. Ford, and B. R.

Chapman. USDA Forest Service and the Nature Conservancy, Durham, North Carolina.

Desrosiers, N., R. Morin, and **J. Jutras.** 2002. Atlas des micromammifères du Québec. Société de la faune et des parcs du Québec, Quebec City, Quebec. 92 pages.

Dobbyn, J. S. 1994. Atlas of the Mammals of Ontario. Federation of Ontario Naturalists, Don Mills, Ontario. 120 pages.

Fauteux, D., L. Imbeau, P. Drapeau, and **M. J. Mazerolle.** 2012. Small mammal responses to coarse woody debris distribution at different spatial scales in managed and unmanaged boreal forests. Forest Ecology and Management 266: 194–205.

Gaudin, T. J., A. N. Miller, J. L. Bramblett, and **T. P. Wilson.** 2011. Holocene and late Pleistocene bat fossils (Mammalia: Chiroptera) from Hamilton County, TN, and their ecological implications. Southeastern Naturalist 10: 609–628.

Glass, B. P., and **M. L. Thies.** 1997. A Key to the Skulls of North American Mammals. Third edition. Sam Houston State University, Hunstville, Texas. 97 pages.

Grayson, D. K., C. Maser, and **Z. Maser.** 1990. Enamel thickness of rooted and rootless microtine molars. Canadian Journal of Zoology 68: 1315–1317.

Hallet, J. G. 1978. *Parascalops breweri*. Mammalian Species 98: 1–4.

Hoofer, S. R., R. A. V. D. Bussche, and **I. Horáček.** 2006. Generic status of the American pipistrelles (Vespertilionidae) with description of a new genus. Journal of Mammalogy 87: 981–992.

ITIS. 2013. Integrated Taxonomic Information System. U.S. Geological Survey. http://www.itis.gov. (Accessed 27 October 2013).

Khalafalla, S. M., and **C. A. Iudica.** 2010. Barn and Long-Eared Owl diets: a comparative study from central Pennsylvania and a key for identification of prey items. Northeastern Naturalist 17: 147–154.

Klingener, D. 1963. Dental evolution of *Zapus*. Journal of Mammalogy 44: 248–260.

Lupien, G. 2001. Recueil photographique des caractéristiques morphologiques servant à l'identification des micromammifères du Québec: volume I – insectivores. Société de la Faune et des Parcs du Québec, Jonquière, Québec. 23 pages.

Lupien, G. 2002. Recueil photographique des caractéristiques morphologiques servant à l'identification des micromammifères du Québec: volume II – rongeurs. Société de la Faune et des Parcs du Québec, Jonquière, Québec. 26 pages.

Lyman, R. L. 2008. Quantitative paleozoology. Cambridge University Press, New York, New York. 372 pages.

Mayhew, D. F. 1977. Avian predators as accumulators of fossil mammal material. Boreas 6: 25–31.

Merritt, J. F. 2010. The Biology of Small Mammals. Johns Hopkins University Press, Baltimore, Maryland. 313 pages.

Mollhagen, T. R., R. W. Wiley, and **R. L. Packard.** 1972. Prey remains in Golden Eagle nests: Texas and New Mexico. Journal of Wildlife Management 36: 784–792.

Nagorsen, D. W. 2002. An Identification Manual to the Small Mammals of British Columbia. British Columbia Ministry of Sustainable Resource Management, Victoria, British Columbia. 153 pages.

Naughton, D. 2012. The Natural History of Canadian Mammals. Canadian Museum of Nature, Ottawa, Ontario, and University of Toronto Press, Toronto, Ontario. 824 pages.

Oksanen, T., L. Oksanen, and **S. D. Fretwell.** 1985. Surplus killing in the hunting strategy of small predators. American Naturalist 126: 328–346.

Peterson, R. L. 1966. The Mammals of Eastern Canada. Oxford University Press, Toronto, Ontario. 465 pages.

Phillips, C. J., and **B. Oxberry.** 1972. Comparative histology of molar dentitions of *Microtus* and *Clethrionomys*, with comments on dental evolution in microtine rodents. Journal of Mammalogy 53: 1–20.

Repenning, C. A. 1967. Subfamilies and Genera of the Soricidae. United States Department of the Interior, Washington, D.C. 74 pages.

Rich, S. M., C. W. Kilpatrick, J. L. Shippee, and **K. L. Crowell.** 1996. Morphological differentiation and identification of *Peromyscus leucopus* and *P. maniculatus* in Northeastern North America. Journal of Mammalogy 77: 985–991.

Roest, A. I. 1991. Key-Guide to Mammal Skulls and Lower Jaws. Mad River Press, Eureka, California. 39 pages.

Séguy, M. 2010. Les habitudes alimentaires de la petite nyctale (*Aegolius acadicus*) en sapinière à bouleau blanc du Québec. Master's thesis, Université Paul Cézanne, Marseille, France.

van Zyll de Jong, C. G. 1983. Traité des mammifères du Canada. 1. Les marsupiaux et les insectivores. Musée national des sciences naturelles, Ottawa, Ontario. 217 pages.

Wilson, D. E., and **D. M. Reeder.** 2005. Mammal Species of the World. Third edition. http://vertebrates.si.edu/msw/mswCFApp/msw/index.cfm. (Accessed 27 October 2013).

Yates, T. L., and **D. J. Schmidly.** 1978. *Scalopus aquaticus*. Mammalian Species 105: 1–4.

Supplementary material available at:
http://www.canadianfieldnaturalist.ca

Received 9 January 2013
Accepted 8 April 2013

Glossary of terms

Alveolus	Socket in which the roots of a tooth are set (Figures 24, 25, and 28) (*alv*).
Angular process	Posterior and ventral-most bony projection of the mandible; the angular process is posterior to the coronoid process (Figures 1 and 24) (*ang*).
Anteroconid	Anterior-most cusp on the m1 of jumping mice (Figure 19) (*antc*).
Anteromedian fold	Concave fold created by the anteroconid on the anterior part of m1 (*antf*).
Anteroposterior length	Length in the direction of the mandibular tooth row.
Brachydont tooth	Closed-rooted tooth with determinate growth (Figures 22 and 23).
Condyle/condylar process	Bony projection located on the ramus between the coronoid and the angular process (Figures 1 and 24) (*con*).
Coronoid process	Posterior and dorsal-most bony projection of the mandible; the coronoid process is anterior to the angular process (Figures 1 and 24) (*cor*).
Closed triangle (of enamel)	In rodents, the external layer of molars that forms occlusal triangular shapes (Figures 16 and 21) (*ct*).
Mandibular foramen	Small hole located below the temporal fossa and serves as a canal for the dental nerve.
Dentary bone	One side (half) of the mandible.
Diastema (plural: diastemata)	Space between two adjacent teeth (Figure 2) (*dia*).
Enamel	The hard external layer of the tooth.
Horizontal ramus	The anterior part of the dentary that supports the teeth (Figure 1B) (*hra*).
Hypoconid	The most posterior cusp (Figure 24).
Hypsodont tooth	Continually growing tooth. The enamel typically covers most of the tooth. Teeth are rootless (Figures 22 and 23).
Interdenticular space	Space between the cusps present on the incisors of shrews (Figure 30).
Labial	Next to the lips.
Labiolingual width	Length of teeth in the direction perpendicular to the mandibular tooth row.
Length of the mandibular tooth row	Length of the lower tooth row (c1–m3) (Figures 1, 6, 33, 37, and 42).
Lingual	Next to the tongue; the interior of the mouth.
Mandible	Both dentary bones, often referred as the lower jaw (*ma*).
Mandibular tooth row	All contiguous teeth of one dentary bone (*mt*). In Carnivora, Chiroptera, and Soricimorpha, all teeth form the toothrow. In Rodentia and Lagomorpha, premolars and molars form the toothrow.
Mental foramen	Small hole located on the labial face of the horizontal ramus (Figure 24).
Metaconid	Cusp posterior to the anteroconid on the lingual side of m1 in jumping mice.
Occlusal	The side of the teeth which meets with the opposing teeth.
Paraconid	Anterior-most cusp on molars in lateral view (Figure 24).
Pigmentation	Coloration of the teeth (*pg*). It is often dark in shrews.
Postmandibular foramen	Small hole next to the mandibular foramen that connects with the temporal fossa (Figure 30).
Premetaconid fold	Small depression, resembling a trench, separating the anteroconid from the metaconid on the molars of jumping mice (Figure 19) (*prmf*).
Protoconid	Middle cusp on the molars of shrews in lateral view (Figures 19 and 24).
Re-entrant angles	Inward pointing angle defined by the margin of the prismatic molars in voles (Figures 16 and 21) (*ra*).
Temporal fossa	Large opening on the lingual side of the vertical ramus.
Vertical ramus	The posterior part of the dentary, composed of the coronoid, condylar, and angular processes (Figure 1B) (*vra*).

Key to the mandibles of small mammals of eastern Canada

(full key illustrated with pictures provided in Supplementary material available at: http://www.canadianfield naturalist.ca)

A. General key to small mammals

1a. Wide diastema between the incisor and molars (Figure 2A) 2
1b. No diastema between the incisor and molars (Figure 2B) 3

2a. Two premolars and three molars; coronoid process and condylar process not differentiated or coronoid process minute (Figure 3A) . . . . Lagomorpha (section B) 5
2b. One premolar or none and three molars; coronoid process clearly differentiated from the condylar process (Figure 3B) . . . . Rodentia (section C) 7

3a. Canines and premolars similar in size; well-developed angular process that is often the most posterior part of the dentary bone (Figure 4A) . . . . Soricomorpha (section D) 31
3b. Canines two to three times the size of the adjacent premolar; small but robust angular process . . . . (Figure 4B) 4

4a. The most posterior molar often much smaller than the most anterior molar; lower edge of ramus without a bump under the canine; height of the coronoid process much higher than the height of the condylar process (Figure 5A) . . . . Carnivora (section E) 42
4b. Three W-shaped molars of similar size; lower edge of ramus with a bump under the canine; height of the coronoid process similar in size to or slightly higher than the height of the condylar process (Figure 5B) . . . . Chiroptera (section F) 50

B. Lagomorpha (Leporidae)

5a. Height of coronoid process >40 mm; length of mandibular tooth row >16 mm (Figure 6A) . . . . *Lepus arcticus*, *L. townsendii*, *L. europaeus*
5b. Height of coronoid process <40 mm; length of mandibular tooth row <16 mm (Figure 6B) 6

6a. Mental foramen easily visible from the occlusal view (Figure 7A) . . . . *Sylvilagus floridanus*
6b. Mental foramen barely visible from the occlusal view (Figure 7B) . . . . *Lepus americanus*

C. Rodentia (Cricetidae, Dipodidae, Erethizontidae, Muridae, and Sciuridae)

7a. Lower edge of horizontal ramus with sharp angle under p1 (Figure 8A); angular process clearly smaller than the coronoid process; cheek teeth with closed circular patterns of enamel (Figure 8B) . . . . *Erethizon dorsatum*
7b. Lower edge of horizontal ramus smooth; the coronoid process and the angular process are similar in size or the angular process is larger than the coronoid process; cheek teeth with triangular patterns of enamel or without clearly defined patterns 8

8a. Angular process clearly the most exterior part of the mandible (Figure 9A); angular process about twice as wide labially as the condylar process (Figure 9A); anterior edge of the coronoid process that connects with the angular process creates a bump pointing outwards at the level of p1-m1 in the occlusal view (Figure 9B); . . . . *Marmota monax*
8b. The condylar process or the coronoid process is the most exterior part of the mandible (occlusal view); no bumps created by the edge of the coronoid and angular processes next to p1-m1; angular process about the same labial thickness or less than the condylar process 9

9a. Tip of the angular process clearly higher than the teeth (Figure 10A) . . . . *Ondatra zibethicus*
9b. Tip of the angular process below or even with the teeth (Figure 10B) 10

10a. One premolar (Figure 11A); angular process extends slightly behind the coronoid process (Figure 11C) 11
10b. No premolar (Figure 11B); angular process extends well behind the coronoid process (Figure 11D) 18

11a. Coronoid process long; size of the notch between the coronoid and condylar processes similar in size to the notch between the condylar and angular processes (Figures 12A and 12B) 12
11b. Coronoid process relatively short; size of the notch between the coronoid and condylar processes clearly smaller than the notch between the condylar and angular processes (Figures 12C and 12D) . . 14

12a. T-shaped condylar process; angular and condylar processes equally posterior (Figure 12A) . . . . *Poliocitellus franklinii*
12b. A-shaped condylar process; condylar process clearly the most posterior component of the ramus (Figure 12B) 13

13a. Length of the mandibular tooth row <5.5 mm . . . . *Tamias minimus*
13b. Length of the mandibular toothrow >5.5 mm . . . . *Tamias striatus*

14a. Height of the coronoid process >17 mm; length of the mandibular tooth row >35 mm 15
14b. Height of the coronoid process <17 mm; length of the mandibular tooth row <35 mm 16

15a. Coronoid process short; notch created by the coronoid process and the condylar process appears wide open; lower tip of the angular process appears squared (Figure 13A) . . . . *Sciurus niger*
15b. Coronoid process longer; coronoid notch narrow; lower tip of the angular process appears rounded (Figure 13B) . . . . *Sciurus carolinensis*

16a. Uppermost edge of the condylar process relatively flat (Figure 14A) . . . . *Tamiasciurus hudsonicus*
16b. Uppermost edge of the condylar process concave (Figure 14B) 17

17a. Posterior tip of the angular process above the notch on the lower edge of the horizontal ramus (Figure 15A) . . . . *Glaucomys volans*
17b. Posterior tip of the angular process below or at the same level as the notch on the lower edge of the horizontal ramus (Figure 15B) . . . . *Glaucomys sabrinus*

18a. Molars without re-entrant angles or closed triangles (Figure 16A) 19
18b. Molars with well-defined lingual and labial re-entrant angles (Figure 16B), often with closed triangles of enamel (Figure 16C) 23

19a. Condylar process clearly the most posterior part of the dentary bone; coronoid process small, at about the same height as the condylar process (Figure 17A) . . . . *Peromyscus leucopus* or *P. maniculatus*
19b. Condylar process slightly posterior to the angular process or about equally posterior; coronoid process relatively long and higher than the condylar process (Figure 17B) 20

20a. Molars with complex patterns of enamel loops (Figure 18A) 21
20b. Molars with simple patterns of enamel loops (Figures 18B and 18C) 22

21a. Anteromedian fold present on m1; anteroconid of m1 clearly separated from the protoconid by the preprotoconid and premetaconid folds (Figure 19A) . . . . *Zapus hudsonius*
21b. Anteromedian fold absent on m1; anteroconid of m1 not separated or slightly separated from the protoconid by the premetaconid fold (Figure 19B) . . . . *Napaeozapus insignis*

22a. Molars with simple patterns of enamel (Figure 20A) . . . . *Mus musculus*
22b. Molars with two rows of cusps without patterns of enamel (Figure 20B) . . . . *Rattus norvegicus*

23a. Re-entrant angles of molars much deeper on lingual side than on labial side (Figures 21A, 21B, and 21C) 24
23b. Re-entrant angles of molars equal in size on both lingual and labial side (Figures 21D, 21E, 21F, 21G, 21H, and 21I) 26

24a. Brachydont teeth (molars closed-rooted) (Figures 22A, 22B, 22C, 23A, and 23B); several small closed triangles on the labial side of molars (Figure 21A) . . . . *Phenacomys ungava*
24b. Hypsodont teeth (molars open-rooted) (Figures 22D and 23C); one closed triangle or none on the labial side of each molar (Figures 21B and 21C) 25

25a. A single closed triangle on the labial side of each molar (Figure 21B) . . . . *Synaptomys cooperi*
25b. No closed triangle on the labial side of molars (Figure 21C) . . . . *Synaptomys borealis*

26a. Brachydont teeth (molars closed-rooted) (Figures 22A, 22B, 22C, 23A, and 23B); occlusal triangles of molars rounded and "enclosed" by the enamel borders (Figures 21D and 21E) 27
26b. Hypsodont teeth (molars open-rooted) (Figures 22D and 23C); occlusal closed triangles with sharp tips (Figures 21F, 21G, 21H, and 21I) 28

27a. Occlusal triangular shapes of enamel of m1 and m2 often connected by wide bridges; shape of the anterior triangle of m3 is typically similar to the posterior triangles (Figure 21D) . . . . *Myodes gapperi*
27b. Occlusal triangles on m1 and m2 often connected by narrow bridges; shape of the anterior triangle of m3 often different from the other triangles (Figure 21E) . . . . *Myodes glareolus*

28a. Presence of a small fold of enamel on the anterior and lingual side of m2 (Figure 21F) . . . . *Dicrostonyx hudsonius*
28b. Absence of a small fold of enamel on the anterior and lingual side of m2 (Figures 21G, 21H, and 21I) 29

29a. Three closed triangles on m1 (Figure 21G) . . . . *Microtus pinetorum*
29b. Five closed triangles on m1 (Figures 21H and 21I) 30

30a. Two closed triangles on m2 (Figure 21H) . . . . *Microtus chrotorrhinus*
30b. Four closed triangles on m2 (Figure 21I) . . . . *Microtus pennsylvanicus*

D. Soricomorpha (Soricidae and Talpidae)
31a. Teeth all white; incisors without a posterior cusp; alveolus of incisors does not extend under premolars or molars (Figure 25A) 32
31b. Tip of teeth often with red and/or brown pigments; incisors with a posterior cusp; alveolus of incisors extends beneath the first premolar or posteriorly (Figures 24 and 25B) 34

32a. Two incisors, no canine, and three premolars; presence of a short diastema between the second incisor and the first premolar (Figure 26A) . . . . *Scalopus aquaticus*
32b. Three incisors, one canine, and four premolars; presence of several short diastemata between the premolars (Figure 26B) or complete absence of diastemata (Figure 26C) 33

33a. Canine and the first three premolars separated by short diastemata; angular process long and slender; condylar process about the same height as the coronoid process or higher; coronoid process clearly smaller than the condylar process (Figure 26B) . . . . *Condylura cristata*
33b. Canine and first three premolars not separated by diastemata; coronoid process higher than the condylar process; coronoid larger than the condylar process (Figure 26C) . . . . *Parascalops breweri*

34a. Alveolus of incisor extends slightly or substantially beneath m1; alveolus extends at the level of the m1 paraconid or posteriorly (Figure 27A) 35
34b. Alveolus of incisor does not extend beneath the m1 paraconid (Figure 27B) 36

35b. Three small cusps on the occlusal surface of the incisor; angular process long and very slender (Figure 28A) . . . . *Sorex hoyi*
35a. One or two small cusps on the occlusal surface of the incisor; angular process relatively short and robust (Figure 28B) . . . . *Blarina brevicauda*

36a. Mental foramen located beneath the m1 paraconid; the space between both cusps on the molars is relatively large (Figure 29A) . . . . *Sorex dispar*
36b. Mental foramen located beneath the m1 protoconid or posteriorely; the space between both cusps on the molars is relatively small (Figure 29B) 37

37a. Postmandibular foramen present (Figure 30A); deep interdenticular spaces on i1 (Figure 30B) . . . 38
37b. Postmandibular foramen absent; shallow interdenticular spaces on i1 (Figure 30C) 39

38a. Height of coronoid process <4.5 mm (Figure 24) . . . . . *Sorex maritimensis*
38b. Height of coronoid process >4.5 mm (Figure 24) . . . . . *Sorex arcticus*

39a. Height of coronoid process >4.5 mm (Figure 24) . . . . . *Sorex palustris*
39b. Height of coronoid process <4.5 mm (Figure 24) 40

40a. Height of coronoid process <3.75 mm (Figure 24) . . . . . *Sorex cinereus*
40b. Height of coronoid process >3.75 mm (Figure 24) . . . . . *Sorex fumeus*

E. Carnivora (Canidae, Mephitidae, and Mustelidae)
41a. Two molars; very small to no diastema between c1 and p1; anterior part of the ramus under the canine thick (Figure 31A) 42
41b. Three molars; diastema between c1 and p1 about equal in size to p1 or larger; anterior part of the ramus under the canine slender (Figure 31B) 48

42a. Four premolars (Figure 31A) 43
42b. Three premolars (Figure 32) 44

43a. Length of the mandibular tooth row <38 mm; posterior mental foramen located beneath the hypoconid of p3; coronoid process relatively sharp (Figure 33A) . . . . . *Martes americana*
43b. Length of the mandibular tooth row >38 mm; posterior mental foramen often located beneath the protoconid of p3; coronoid process rounded (Figure 33B) . . . . . *Martes pennanti*

44a. Bump present on the anterior part of the horizontal ramus approximately beneath p1 (Figure 34A); p1 clearly smaller than m2 (Figure 34C) . . . . . *Mephitis mephitis*
44b. Absence of a bump on the anterior part of the horizontal ramus (Figure 34B); p1 larger than m2 or about similar in size (Figure 34D) 45

45a. p2 often with a well-developed paraconid (Figure 35A); posterior edge of the vertical ramus with a distinct convex notch between the coronoid process and the condylar process (Figure 36A) . . . . . *Neovison vison*
45b. p2 often without a small anterior cusp (Figure 35B); posterior edge of the vertical ramus straight between the coronoid process and the condylar process (Figure 36B) 46

46a. Height of coronoid process <7.1 mm; length of mandibular tooth row <10 mm (Figure 37) . . . . . *Mustela nivalis*
46b. Height of coronoid process >7.1 mm; length of mandibular tooth row >10 mm (Figure 37) 47

47a. Height of the coronoid process generally <10.5 mm; length of mandibular tooth row never >16 mm (Figure 37); posterior edge of the vertical ramus between the coronoid process and the condylar process relatively flat (Figure 38A) . . . . . *Mustela erminea*
47b. Height of the coronoid process generally >10.5 mm; length of mandibular tooth row often >16 mm (Figure 37); posterior edge of the vertical ramus between the coronoid process and the condylar process with a convex curve (Figure 38B) . . . . . *Mustela frenata*

48a. Presence of a clearly defined step on the lower edge of the horizontal ramus anterior to the angular process; diastemata between c1 and p1, between p1 and p2, and between p2 and p3 (Figure 39A) . . . . . *Urocyon cinereoargenteus*
48b. Lower edge of the horizontal ramus anterior to the angular process smooth, without a step; only one diastema between c1 and p1 (Figure 39B) 49

49a. Anteroposterior length of the diastema between c1 and p1 smaller than p1 (Figure 40A) . . . *Vulpes lagopus*
49b. Anteroposterior length of the diastema between c1 and p1 about equal to p1 or larger (Figure 40B) . . . . . *Vulpes vulpes*

F. Chiroptera (Vespertilionidae)
50a. Three premolars (Figure 41A) 51
50b. Two premolars (Figure 41B) 54

51a. Mandibular length >11.5 mm (Figure 42); hypoconid of p3 with lingual crest directed medially creating a distinct lingual bulge (Figure 43A) . . . . *Lasionycteris noctivagans*
51b. Mandibular length <11.5 mm (Figure 42); hypoconid of p3 without a distinct lingual bulge (Figure 43B) 52

52a. p3 rectangular, anteroposterior length greater than labiolingual width (Figure 44A); mandibular length generally ≥11mm (Figure 42) . . . . *Myotis septentrionalis*
52b. p3 squared, anteroposterior length approximately equal to labiolingual width (Figure 44B); mandibular length <11mm (Figure 42) 53

53a. Mandibular length generally >10 mm; length of the mandibular tooth row generally >5.5 mm (Figure 42) . . . . *Myotis lucifugus*
53b. Mandibular length generally <10 mm; length of the mandibular tooth row generally <5.5 mm (Figure 42) . . . . *Myotis leibii*

54a. Mandibular length >12.5 mm (Figure 42) 55
54b. Mandibular length <12.5 mm (Figure 42) 56

55a. Mandibular length >14 mm (Figure 42); rounded coronoid process much taller than c1 (Figure 45A); p2 squared, with labiolingual width approximately equal to anteroposterior length (Figure 46A) . . . . *Eptesicus fuscus*
55b. Mandibular length ≤14 mm (Figure 42); sharp coronoid process approximately same height as c1 (Figure 45B); p2 rectangular with labiolingual width greater than anteroposterior length (Figure 46B) . . . . *Lasiurus cinereus*

56a. Length of the mandibular tooth row <5 mm (Figure 42); small diastemata separate i2 from i3, i3 from c1, and p1 from p2; c1 approximately same height as p2 (Figure 47A) . . . . *Perimyotis subflavus*
56b. Length of the mandibular tooth row >5 mm (Figure 42); no diastema between i2 and i3, i3 and c1, or p1 and p2; c1 taller than p2 (Figure 47B) . . . . *Lasiurus borealis*

Key to the mandibles of small mammals of eastern Canada

A. General key to small mammals

1a. Wide diastema between the incisor and molars (Figure 2A) 2
1b. No diastema between the incisor and molars (Figure 2B) 3

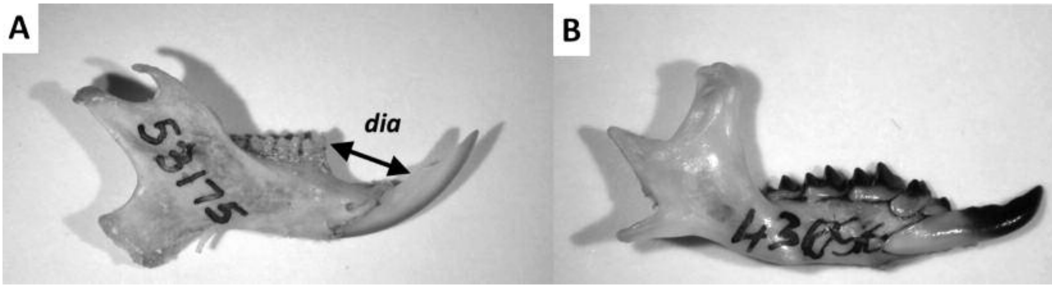

FIGURE 2. (*labial view*) Dentary bone of rodents with a large diastema (*dia*) (*Glaucomys volans*) (A), and soricomorphs (*Blarina brevicauda*) (B).

2a. Two premolars and three molars; coronoid process and condylar process not differentiated or coronoid process minute (Figure 3A) . . . . Lagomorpha (section B) 5
2b. One premolar or none and three molars; coronoid process clearly differentiated from the condylar process (Figure 3B) . . . . Rodentia (section C) 7

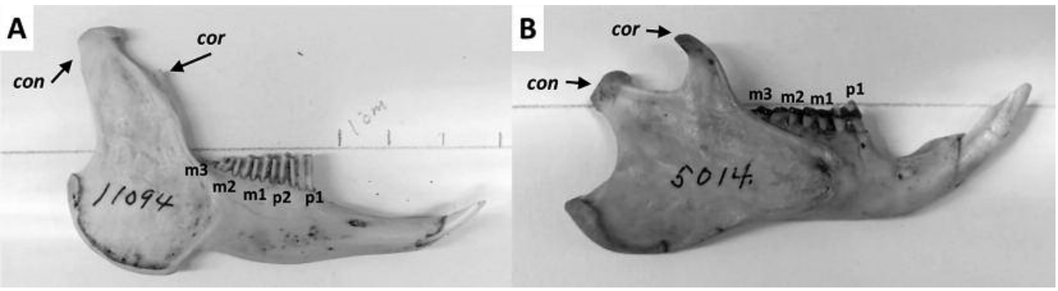

FIGURE 3. (*labial view*) Coronoid (*cor*) and condylar (*con*) processes of lagomorphs (*Lepus arcticus*) (A) and rodents (*Marmota monax*) (B).

3a. Canines and premolars similar in size; well-developed angular process that is often the most posterior part of the dentary bone (Figure 4A) . . . . .Soricomorpha (section D) 31
3b. Canines two to three times the size of the adjacent premolar; small but robust angular process . . . . (Figure 4B) 4

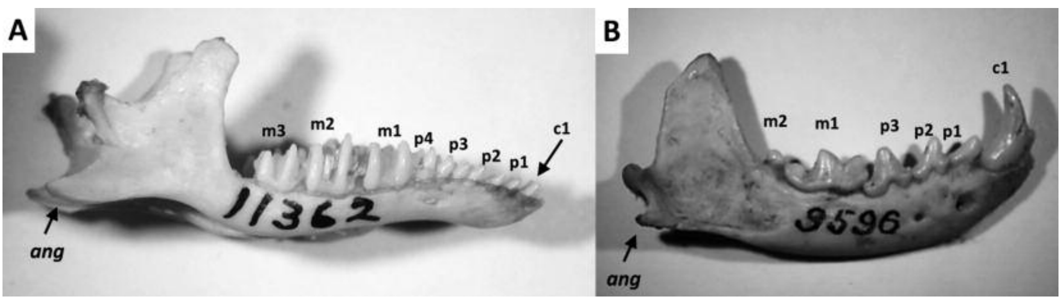

FIGURE 4. (*labial view*) Size of the angular process as well as the size of the canine compared to the adjacent premolar in soricomorphs (*Parascalops breweri*) (A) and carnivores (*Neovison vison*) (B).

4a. The most posterior molar often much smaller than the most anterior molar; lower edge of ramus without a bump under the canine; height of the coronoid process much higher than the height of the condylar process (Figure 5A) . . . . Carnivora (section E) 42
4b. Three W-shaped molars of similar size; lower edge of ramus with a bump under the canine; height of the coronoid process similar in size to or slightly higher than the height of the condylar process (Figure 5B) . . . . Chiroptera (section F) 50

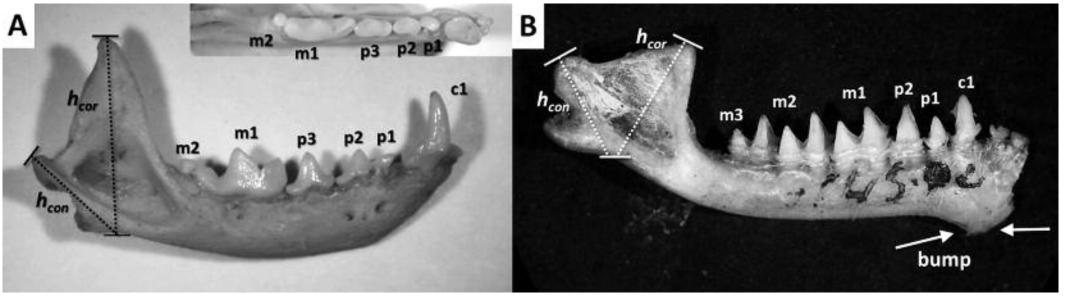

FIGURE 5. (*labial view*) Dentary bones of carnivores (*Mustela erminea*) (A) and chiropterans (*Perimyotis subflavus*) (B) with the height of the condylar process (h_{con}), height of the coronoid process (h_{cor}), and the conspicuous mandibular bump of chiropterans.

B. Lagomorpha (Leporidae)

5a. Height of coronoid process >40 mm; length of mandibular tooth row >16 mm (Figure 6A) . . . . *Lepus arcticus*, *L. townsendii*, *L. europaeus*
5b. Height of coronoid process <40 mm; length of mandibular tooth row <16 mm (Figure 6B) 6

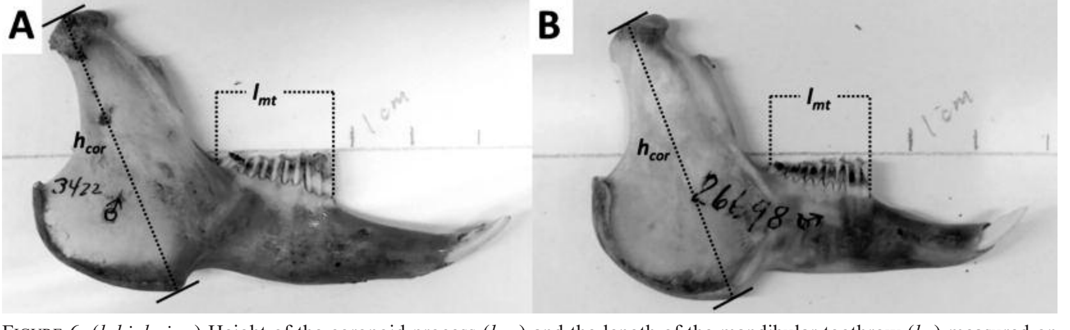

FIGURE 6. (*labial view*) Height of the coronoid process (h_{cor}) and the length of the mandibular toothrow (l_{mt}) measured on lagomorphs (*Lepus townsendii* (A) and *Lepus americanus* (B)).

6a. Mental foramen easily visible from the occlusal view (Figure 7A) . . . . *Sylvilagus floridanus*
6b. Mental foramen barely visible from the occlusal view (Figure 7B) . . . . *Lepus americanus*

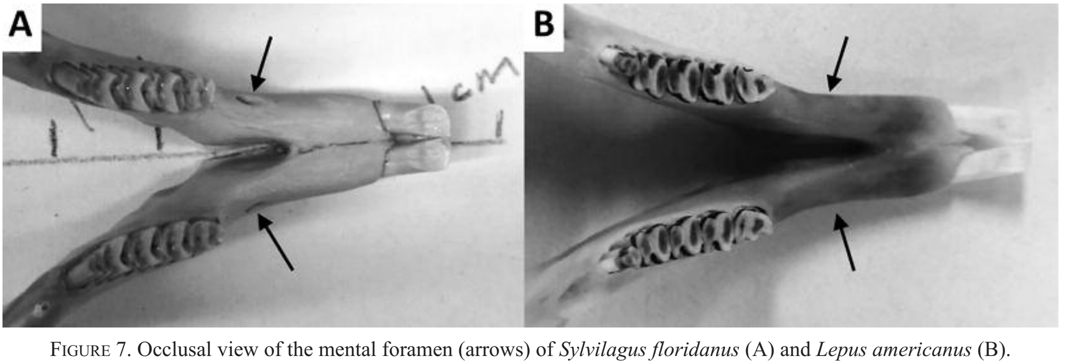

FIGURE 7. Occlusal view of the mental foramen (arrows) of *Sylvilagus floridanus* (A) and *Lepus americanus* (B).

C. Rodentia (Cricetidae, Dipodidae, Erethizontidae, Muridae, and Sciuridae)

7a. Lower edge of horizontal ramus with sharp angle under p1 (Figure 8A); angular process clearly smaller than the coronoid process; cheek teeth with closed circular patterns of enamel (Figure 8B) . . . . *Erethizon dorsatum*

7b. Lower edge of horizontal ramus smooth; the coronoid process and the angular process are similar in size or the angular process is larger than the coronoid process; cheek teeth with triangular patterns of enamel or without clearly defined patterns 8

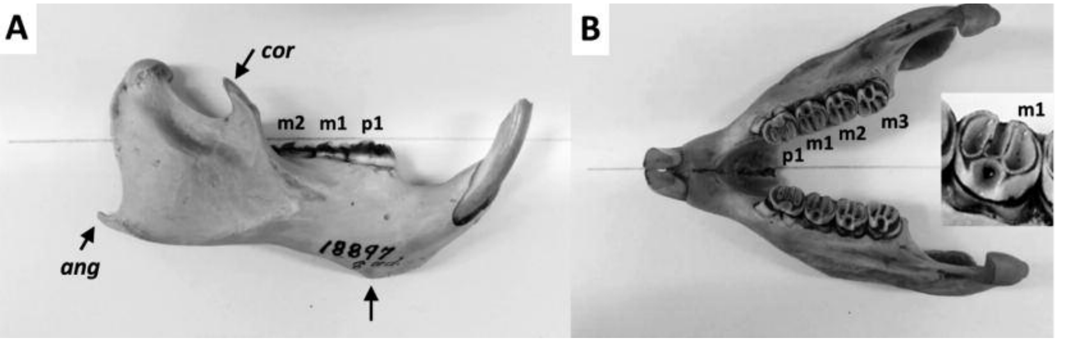

FIGURE 8. Labial view (A) and occlusal view (B) of the *Erethizon dorsatum* mandible. The angular (*ang*) and coronoid (*cor*) processes are indicated by the arrows.

8a. Angular process clearly the most exterior part of the mandible (Figure 9A); angular process about twice as wide labially as the condylar process (Figure 9A); anterior edge of the coronoid process that connects with the angular process creates a bump pointing outwards at the level of p1-m1 in the occlusal view (Figure 9B); . . . . *Marmota monax*

8b. The condylar process or the coronoid process is the most exterior part of the mandible (occlusal view); no bumps created by the edge of the coronoid and angular processes next to p1-m1; angular process about the same labial thickness or less than the condylar process 9

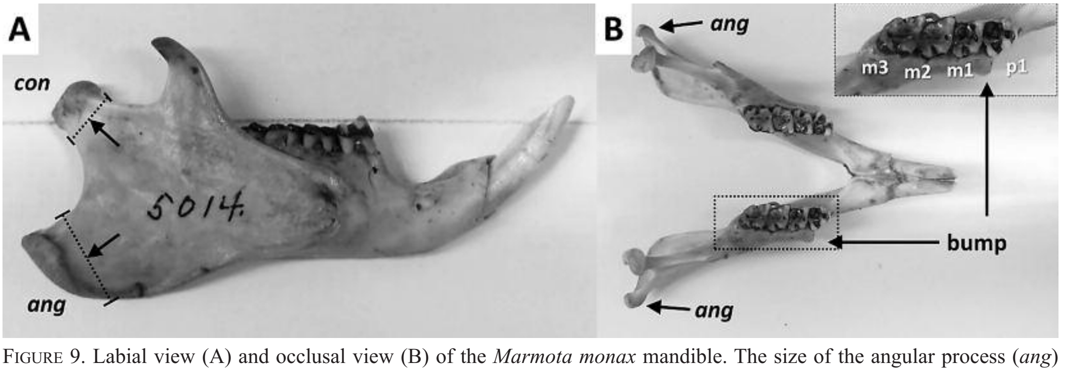

FIGURE 9. Labial view (A) and occlusal view (B) of the *Marmota monax* mandible. The size of the angular process (*ang*) compared to the condylar process (*con*) is shown in A and the bump near p1 and m1 is shown in B.

9a. Tip of the angular process clearly higher than the teeth (Figure 10A) . . . . *Ondatra zibethicus*

9b. Tip of the angular process below or even with the teeth (Figure 10B) 10

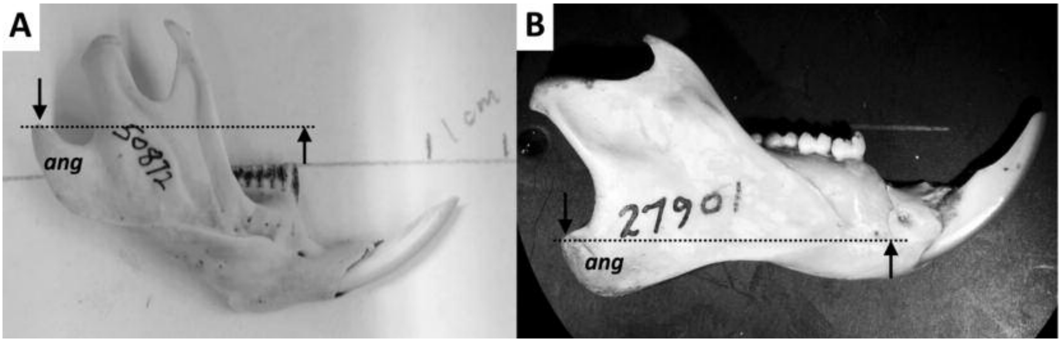

FIGURE 10. (*labial view*) Height of the angular process (arrows) of *Ondatra zibethicus* (A) and sciurids (*Sciurus niger*) (B).

10a. One premolar (Figure 11A); angular process extends slightly behind the coronoid process (Figure 11C) 11
10b. No premolar (Figure 11B); angular process extends well behind the coronoid process (Figure 11D) 18

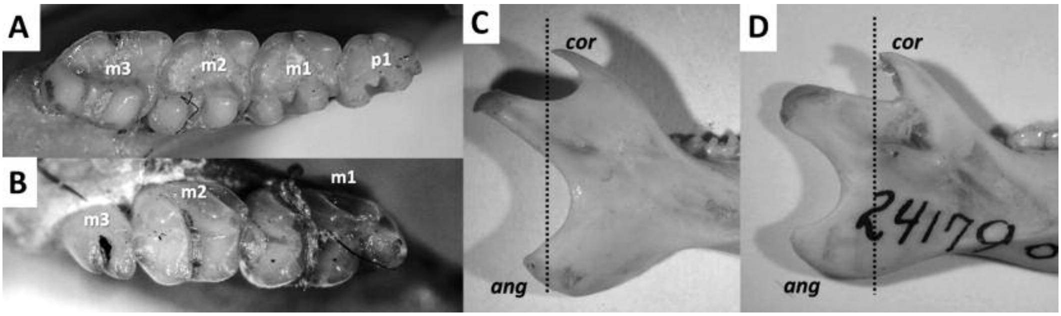

FIGURE 11. (*A and B. occlusal view*; *C and D. labial view*) Dental formula of squirrels (*Glaucomys sabrinus*) (A) and of Cricetidae, Dipodidae, and Muridae (*Mus musculus*) (B) and the angular (*ang*) and coronoid (*cor*) processes of squirrels (*G. sabrinus*) (C) and of other rodents (*Rattus norvegicus*) (D).

11a. Coronoid process long; size of the notch between the coronoid and condylar processes similar in size to the notch between the condylar and angular processes (Figures 12A and 12B) 12
11b. Coronoid process relatively short; size of the notch between the coronoid and condylar processes clearly smaller than the notch between the condylar and angular processes (Figures 12C and 12D) . . 14

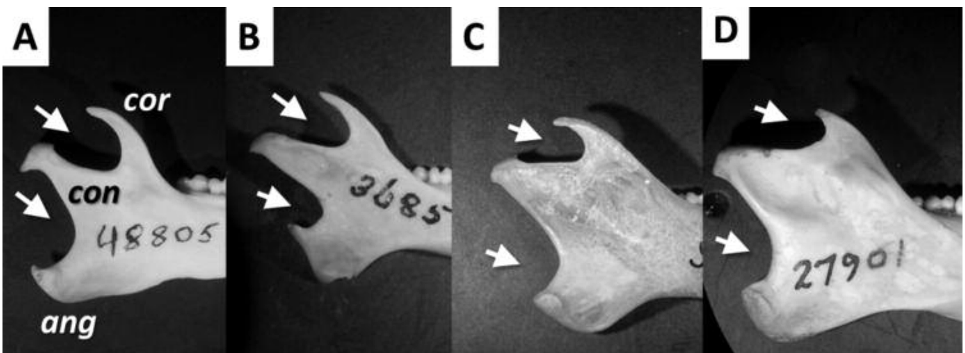

FIGURE 12. (*labial view*) Notches (arrows) created by the coronoid (*cor*), condylar (*con*), and angular (*ang*) processes of *Poliocitellus franklinii* (A), *Tamias minimus* (B), *Tamiasciurus hudsonicus* (C), and *Sciurus niger* (D).

12a. T-shaped condylar process; angular and condylar processes equally posterior (Figure 12A) . . . . *Poliocitellus franklinii*
12b. A-shaped condylar process; condylar process clearly the most posterior component of the ramus (Figure 12B) 13

13a. Length of the mandibular tooth row <5.5 mm . . . . *Tamias minimus*
13b. Length of the mandibular toothrow >5.5 mm . . . . *Tamias striatus*

14a. Height of the coronoid process >17 mm; length of the mandibular tooth row >35 mm 15
14b. Height of the coronoid process <17 mm; length of the mandibular tooth row <35 mm 16

15a. Coronoid process short; notch created by the coronoid process and the condylar process appears wide open; lower tip of the angular process appears squared (Figure 13A) . . . . *Sciurus niger*
15b. Coronoid process longer; coronoid notch narrow; lower tip of the angular process appears rounded (Figure 13B) . . . . *Sciurus carolinensis*

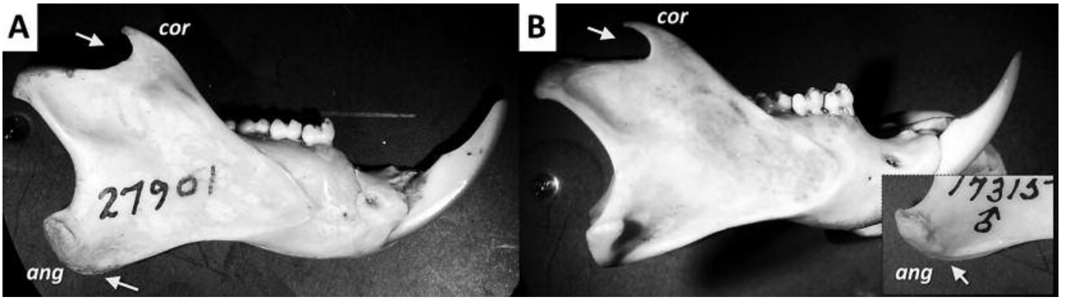

FIGURE 13. (*labial view*) Notches created by the coronoid (*cor*) and the condylar (*con*) processes as well as the shape of the lower part of the angular process of *Sciurus niger* (A) and *S. carolinensis* (B).

16a. Uppermost edge of the condylar process relatively flat (Figure 14A) . . . . *Tamiasciurus hudsonicus*
16b. Uppermost edge of the condylar process concave (Figure 14B) 17

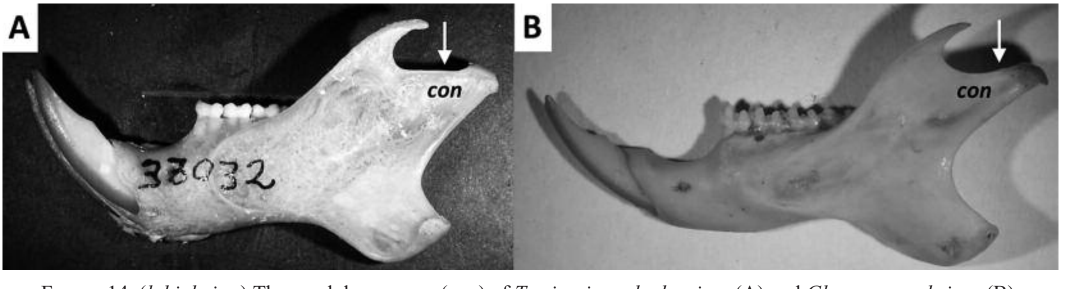

FIGURE 14. (*labial view*) The condylar process (*con*) of *Tamiasciurus hudsonicus* (A) and *Glaucomys sabrinus* (B).

17a. Posterior tip of the angular process above the notch on the lower edge of the horizontal ramus (Figure 15A) . . . . *Glaucomys volans*
17b. Posterior tip of the angular process below or at the same level as the notch on the lower edge of the horizontal ramus (Figure 15B) . . . . *Glaucomys sabrinus*

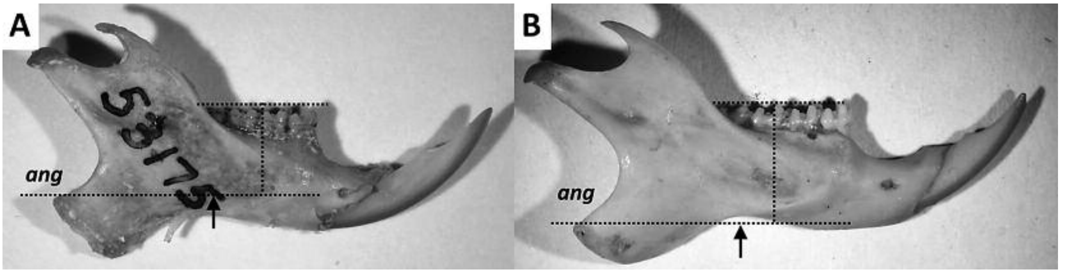

FIGURE 15. (*labial view*) Relative position of the upper part of the angular process (*ang*) in relation to the notch created by the lower edge of the ramus of *Glaucomys volans* (A) and *G. sabrinus* (B).

18a. Molars without re-entrant angles or closed triangles (Figure 16A) 19
18b. Molars with well-defined lingual and labial re-entrant angles (Figure 16B), often with closed triangles of enamel (Figure 16C) 23

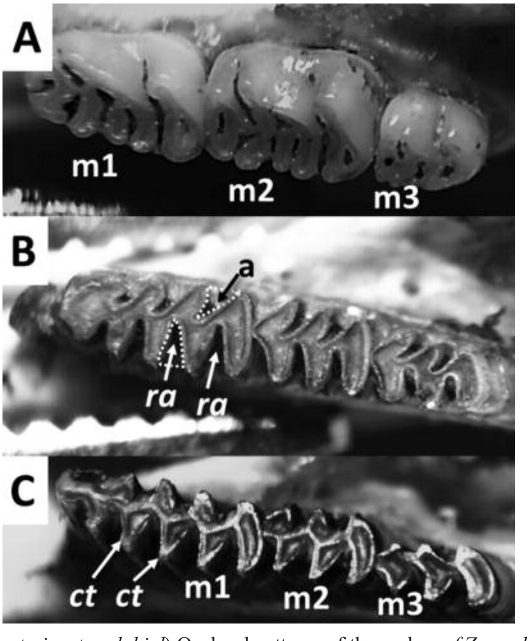

FIGURE 16. (*occlusal view*; *left: anterior*; *top: labial*) Occlusal patterns of the molars *of Zapus hudsonius* (A), *Myodes gapperi* (B), and *Microtus pennsylvanicus* (C). The labels refer to re-entrant angles (*ra*) and closed triangles of enamel (*ct*).

19a. Condylar process clearly the most posterior part of the dentary bone; coronoid process small, at about the same height as the condylar process (Figure 17A) . . . . *Peromyscus leucopus* or *P. maniculatus*
19b. Condylar process slightly posterior to the angular process or about equally posterior; coronoid process relatively long and higher than the condylar process (Figure 17B) 20

20a. Molars with complex patterns of enamel loops (Figure 18A) 21
20b. Molars with simple patterns of enamel loops (Figures 18B and 18C) 22

21a. Anteromedian fold present on m1; anteroconid of m1 clearly separated from the protoconid by the preprotoconid and premetaconid folds (Figure 19A) . . . . *Zapus hudsonius*
21b. Anteromedian fold absent on m1; anteroconid of m1 not separated or slightly separated from the protoconid by the premetaconid fold (Figure 19B) . . . . *Napaeozapus insignis*

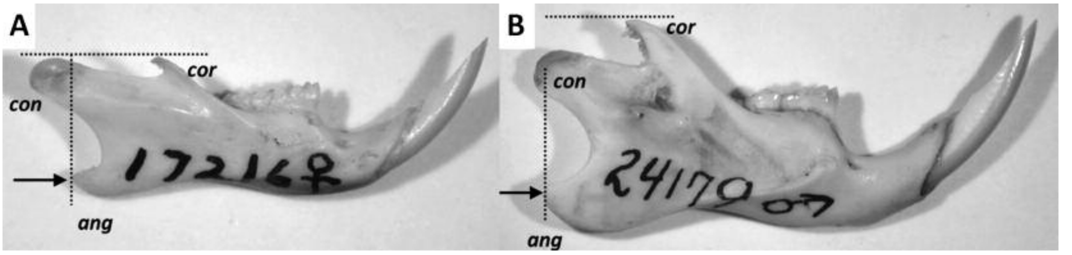

FIGURE 17. (*labial view*) Relative shape, size, and position of the coronoid (*cor*), condylar (*con*), and angular (*ang*) processes of *Peromyscus leucopus* (A) and *Rattus norvegicus* (B).

22a. Molars with simple patterns of enamel (Figure 20A) . . . . *Mus musculus*
22b. Molars with two rows of cusps without patterns of enamel (Figure 20B) . . . . *Rattus norvegicus*

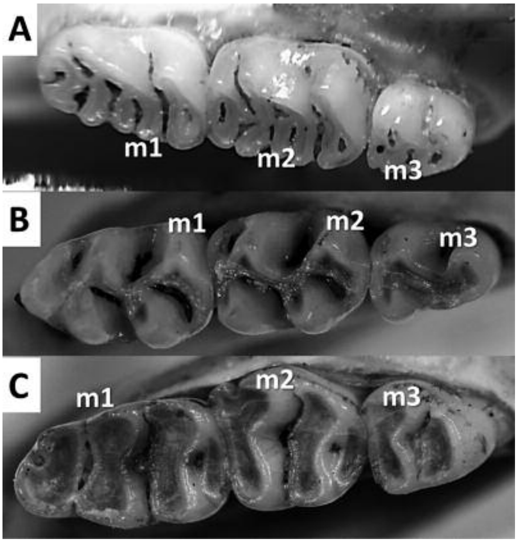

FIGURE 18. (*occlusal view*; *left: anterior*; *top: labial*) Occlusal patterns of the molars of *Zapus hudsonius* (A), *Mus musculus* (B), and *Rattus norvegicus* (C).

23a. Re-entrant angles of molars much deeper on lingual side than on labial side (Figures 21A, 21B, and 21C) 24
23b. Re-entrant angles of molars equal in size on both lingual and labial side (Figures 21D, 21E, 21F, 21G, 21H, and 21I) 26

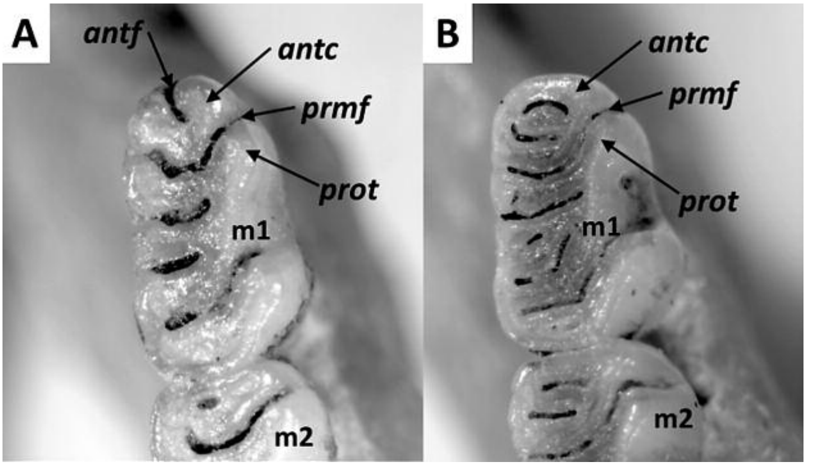

FIGURE 19. (*occlusal view*; *left: lingual*; *top: anterior*) Occlusal pattern of m1 in *Zapus hudsonius* (A) and *Napaeozapus insignis* (B). The labels refer to the anteromedian fold (*antf*), the anteroconid (*antc*), the premetaconid fold (*prmf*), and the protoconid (*prot*).

24a. Brachydont teeth (molars closed-rooted) (Figures 22A, 22B, 22C, 23A, and 23B); several small closed triangles on the labial side of molars (Figure 21A) . . . . *Phenacomys ungava*
24b. Hypsodont teeth (molars open-rooted) (Figures 22D and 23C); one closed triangle or none on the labial side of each molar (Figures 21B and 21C) 25

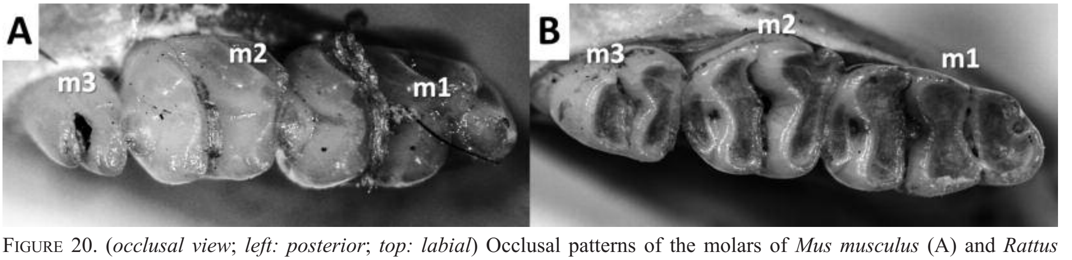

FIGURE 20. (*occlusal view*; *left: posterior*; *top: labial*) Occlusal patterns of the molars of *Mus musculus* (A) and *Rattus norvegicus* (B).

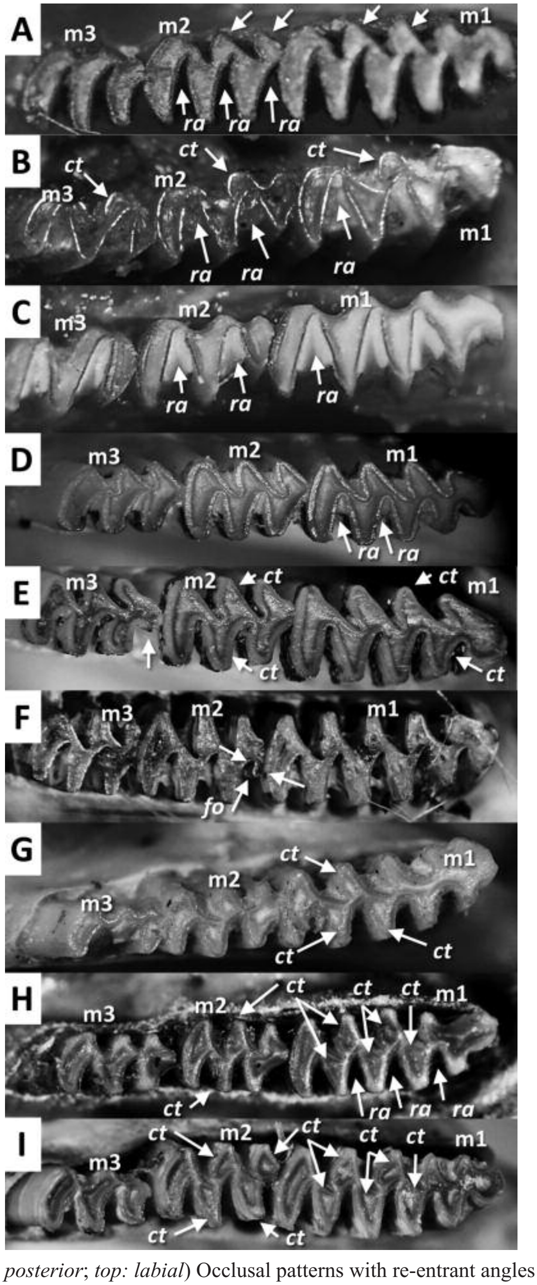

FIGURE 21. (*occlusal view*; *left: posterior*; *top: labial*) Occlusal patterns with re-entrant angles (*ra*), closed triangles (*ct*) and folds of enamel (*fo*) of the molars of *Phenacomys ungava* (A), *Synaptomys cooperi* (B), *Synaptomys borealis* (C), *Myodes gapperi* (D), *Myodes glareolus* (E), *Dicrostonyx hudsonius* (F), *Microtus pinetorum* (G), *Microtus chrotorrhinus* (H), and *Microtus pennsylvanicus* (I).

25a. A single closed triangle on the labial side of each molar (Figure 21B) . . . . *Synaptomys cooperi*
25b. No closed triangle on the labial side of molars (Figure 21C) . . . . *Synaptomys borealis*

26a. Brachydont teeth (molars closed-rooted) (Figures 22A, 22B, 22C, 23A, and 23B); occlusal triangles of molars rounded and "enclosed" by the enamel borders (Figures 21D and 21E) 27
26b. Hypsodont teeth (molars open-rooted) (Figures 22D and 23C); occlusal closed triangles with sharp tips (Figures 21F, 21G, 21H, and 21I) 28

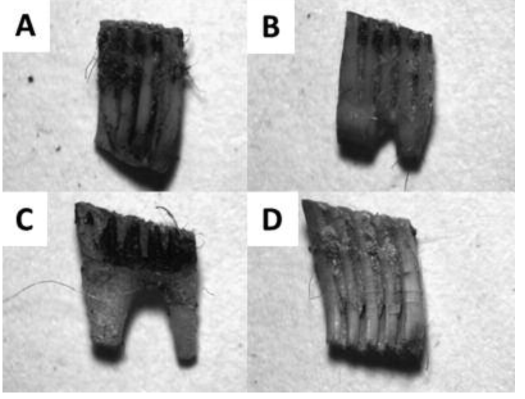

FIGURE 22. (*labial view*) Brachydont teeth in their early stages (*Myodes gapperi*) (A), middle stages (*M. gapperi*) (B), and late stages (*Phenacomys ungava*) (C) and hypsodont teeth (*Microtus pennsylvanicus*) (D).

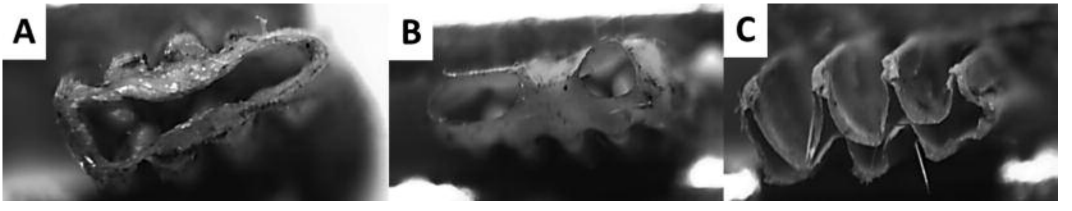

FIGURE 23. (*bottom view*) Base of brachydont teeth in their early stages (*Myodes gapperi*) (A) and middle stages (*M. gapperi*) (B) and of hypsodont teeth (*Microtus pennsylvanicus*) (C).

27a. Occlusal triangular shapes of enamel of m1 and m2 often connected by wide bridges; shape of the anterior triangle of m3 is typically similar to the posterior triangles (Figure 21D) . . . . *Myodes gapperi*
27b. Occlusal triangles on m1 and m2 often connected by narrow bridges; shape of the anterior triangle of m3 often different from the other triangles (Figure 21E) . . . . *Myodes glareolus*

28a. Presence of a small fold of enamel on the anterior and lingual side of m2 (Figure 21F) . . . . *Dicrostonyx hudsonius*
28b. Absence of a small fold of enamel on the anterior and lingual side of m2 (Figures 21G, 21H, and 21I) 29

29a. Three closed triangles on m1 (Figure 21G) . . . . *Microtus pinetorum*
29b. Five closed triangles on m1 (Figures 21H and 21I) 30

30a. Two closed triangles on m2 (Figure 21H) . . . . *Microtus chrotorrhinus*
30b. Four closed triangles on m2 (Figure 21I) . . . . *Microtus pennsylvanicus*

D. Soricomorpha (Soricidae and Talpidae)

31a. Teeth all white; incisors without a posterior cusp; alveolus of incisors does not extend under premolars or molars (Figure 25A) 32
31b. Tip of teeth often with red and/or brown pigments; incisors with a posterior cusp; alveolus of incisors extends beneath the first premolar or posteriorly (Figures 24 and 25B) 34

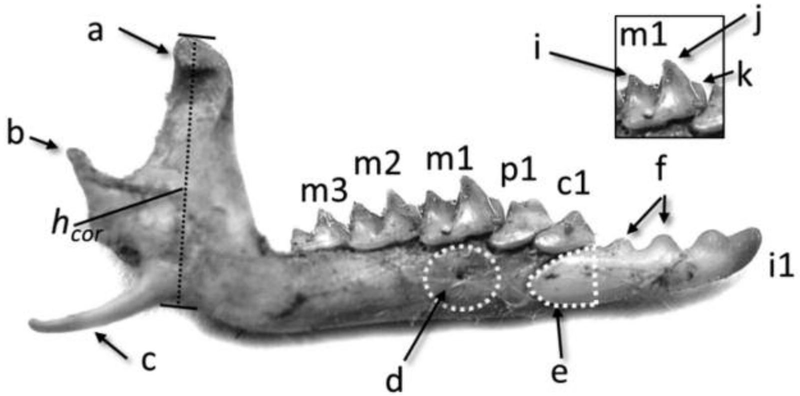

FIGURE 24. (*labial view*) Schematic overview of the shrew dentary bone: coronoid process (a), condylar process (b), angular process (c), mental foramen (d), alveolus of the incisor (e), posterior cusp of the incisor (f), hypoconid (i), protoconid (j), paraconid (k), and height of the coronoid process (h_{cor}).

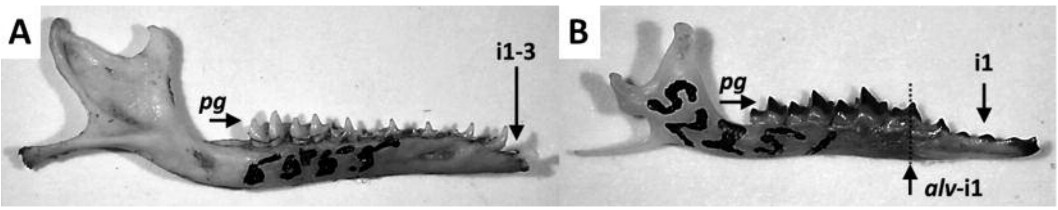

FIGURE 25. (*labial view*) Dentary bones of moles (A) and shrews (B). The labels are as follows: pigmentation (*pg*) and alveolus of the incisor (*alv*-i1). The depth of the incisor alveolus in relation to p1 is shown in B (arrow).

32a. Two incisors, no canine, and three premolars; presence of a short diastema between the second incisor and the first premolar (Figure 26A) . . . . *Scalopus aquaticus*
32b. Three incisors, one canine, and four premolars; presence of several short diastemata between the premolars (Figure 26B) or complete absence of diastemata (Figure 26C) 33

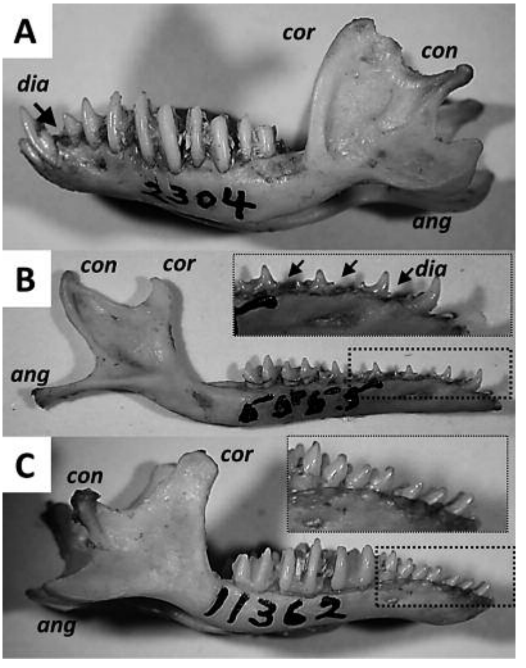

FIGURE 26. (*labial view*) Dentary bones of the three moles (Talpidae) present in eastern Canada: *Scalopus aquaticus* (A), *Condylura cristata* (B), and *Parascalops breweri* (C). The labels refer to the coronoid process (*cor*), condylar process (*con*), angular process *(ang*), and diastema (*dia*).

33a. Canine and the first three premolars separated by short diastemata; angular process long and slender; condylar process about the same height as the coronoid process or higher; coronoid process clearly smaller than the condylar process (Figure 26B) . . . . *Condylura cristata*
33b. Canine and first three premolars not separated by diastemata; coronoid process higher than the condylar process; coronoid larger than the condylar process (Figure 26C) . . . . *Parascalops breweri*

34a. Alveolus of incisor extends slightly or substantially beneath m1; alveolus extends at the level of the m1 paraconid or posteriorly (Figure 27A) 35
34b. Alveolus of incisor does not extend beneath the m1 paraconid (Figure 27B) 36

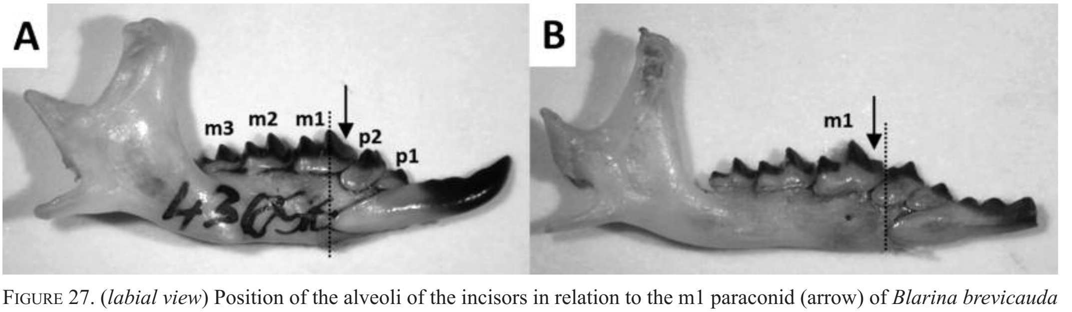

FIGURE 27. (*labial view*) Position of the alveoli of the incisors in relation to the m1 paraconid (arrow) of *Blarina brevicauda* (A) and *Sorex hoyi* (B).

35b. Three small cusps on the occlusal surface of the incisor; angular process long and very slender (Figure 28A) . . . . *Sorex hoyi*
35a. One or two small cusps on the occlusal surface of the incisor; angular process relatively short and robust (Figure 28B) . . . . *Blarina brevicauda*

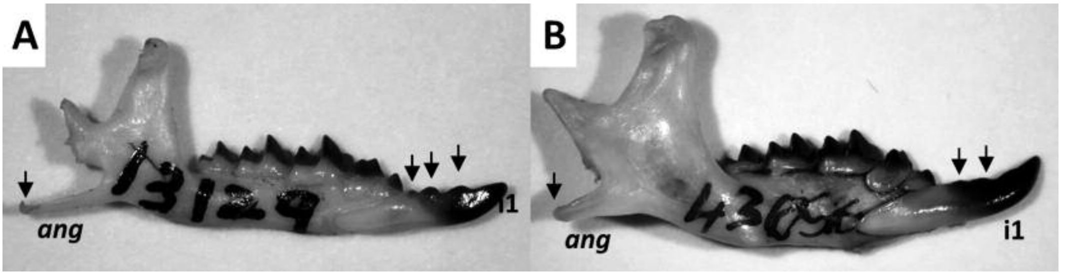

FIGURE 28. (*labial view*) Occlusal cusps on the incisor and the angular process (*ang*) of *Sorex hoyi* (A) and *Blarina brevicauda* (B).

36a. Mental foramen located beneath the m1 paraconid; the space between both cusps on the molars is relatively large (Figure 29A) . . . . *Sorex dispar*
36b. Mental foramen located beneath the m1 protoconid or posteriorely; the space between both cusps on the molars is relatively small (Figure 29B) 37

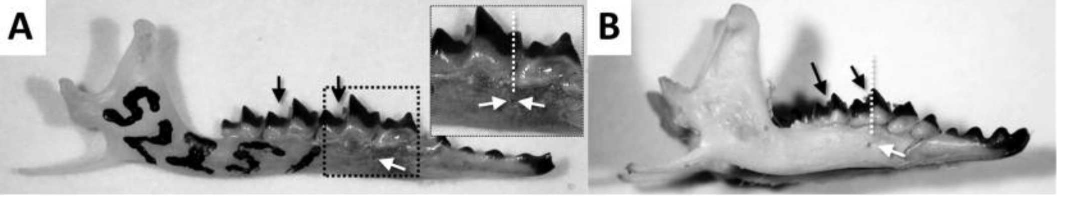

FIGURE 29. (*labial view*) Space between the cusps of molars (black arrows) and the relative position of the mental foramen (white arrows) in relation to the m1 paraconid and protoconid in *Sorex dispar* (A) and *S. maritimensis* (B).

37a. Postmandibular foramen present (Figure 30A); deep interdenticular spaces on i1 (Figure 30B) . . . 38
37b. Postmandibular foramen absent; shallow interdenticular spaces on i1 (Figure 30C) 39

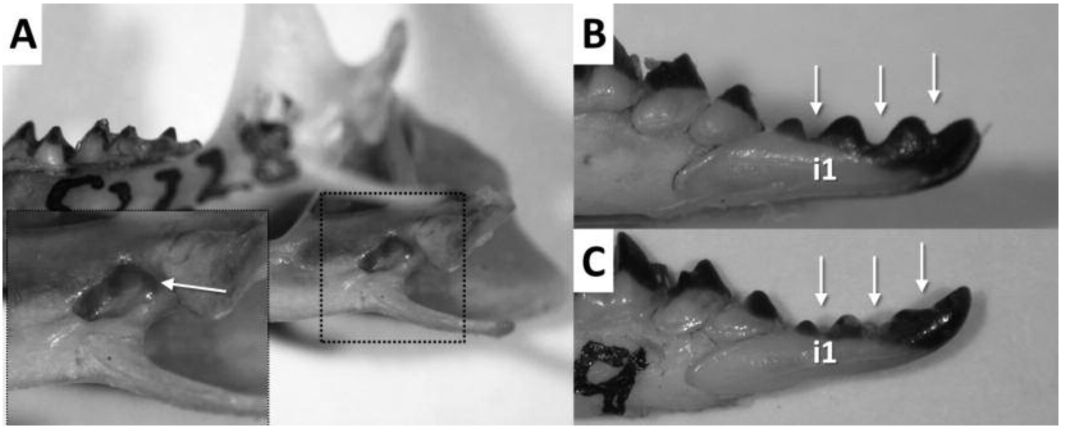

FIGURE 30. (*A. lingual view*; *B. and C. labial view*) Postmandibular foramen of *Sorex arcticus* (A) (arrow) as well as the interdenticular spaces (arrows) of the incisor of *S. arcticus* (B) and *S. palustris* (C).

38a. Height of coronoid process <4.5 mm (Figure 24) . . . . *Sorex maritimensis*
38b. Height of coronoid process >4.5 mm (Figure 24) . . . . *Sorex arcticus*

39a. Height of coronoid process >4.5 mm (Figure 24) . . . . *Sorex palustris*
39b. Height of coronoid process <4.5 mm (Figure 24) 40

40a. Height of coronoid process <3.75 mm (Figure 24) . . . . *Sorex cinereus*
40b. Height of coronoid process >3.75 mm (Figure 24) . . . . *Sorex fumeus*

E. Carnivora (Canidae, Mephitidae, and Mustelidae)

41a. Two molars; very small to no diastema between c1 and p1; anterior part of the ramus under the canine thick (Figure 31A) 42

41b. Three molars; diastema between c1 and p1 about equal in size to p1 or larger; anterior part of the ramus under the canine slender (Figure 31B) 48

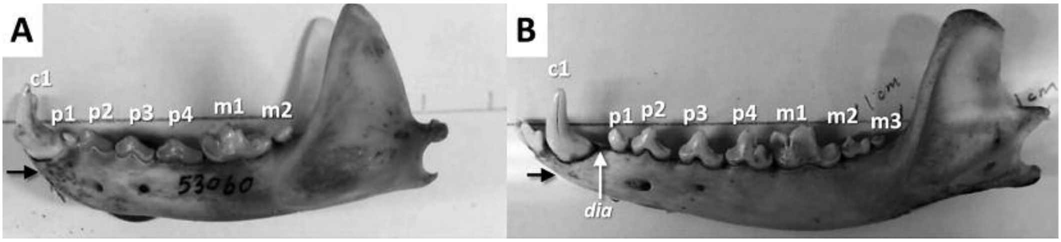

FIGURE 31. (*labial view*) Dental formula of mustelids (*Martes americana*) (A) and canids (*Vulpes lagopus*) (B) as well as the diastema (*dia*) present between c1 and p1 in canids. The black arrow shows the different shapes of the ramus below the canine in both species.

42a. Four premolars (Figure 31A) 43

42b. Three premolars (Figure 32) 44

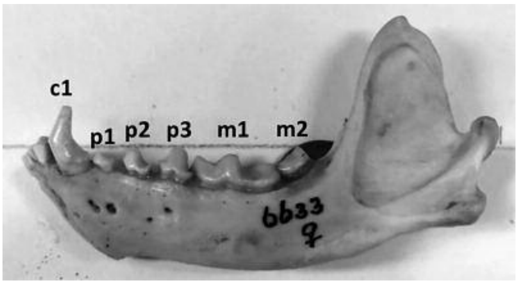

FIGURE 32. (*labial view*) The dentary bone of *Mustela*, *Neovison*, and *Mephitis mephitis* (shown in the figure), all composed of three premolars.

43a. Length of the mandibular tooth row <38 mm; posterior mental foramen located beneath the hypoconid of p3; coronoid process relatively sharp (Figure 33A) . . . . *Martes americana*

43b. Length of the mandibular tooth row >38 mm; posterior mental foramen often located beneath the protoconid of p3; coronoid process rounded (Figure 33B) . . . . *Martes pennanti*

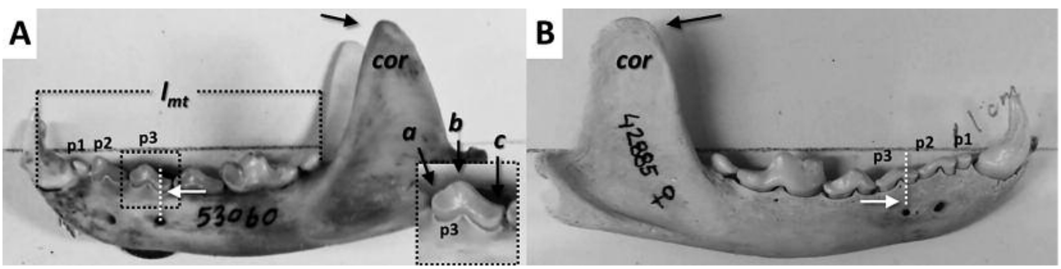

FIGURE 33. (*labial view*) Shape of the coronoid process (black arrow), length of the mandibular tooth row (l_{mt}) and the position of the posterior mental foramen (white arrow) in relation to the paraconid (*a*), the protoconid (*b*), and the hypoconid (*c*) of p3 in *Martes americana* (A) and *M. pennanti* (B).

44a. Bump present on the anterior part of the horizontal ramus approximately beneath p1 (Figure 34A); p1 clearly smaller than m2 (Figure 34C) . . . . *Mephitis mephitis*

44b. Absence of a bump on the anterior part of the horizontal ramus (Figure 34B); p1 larger than m2 or about similar in size (Figure 34D) 45

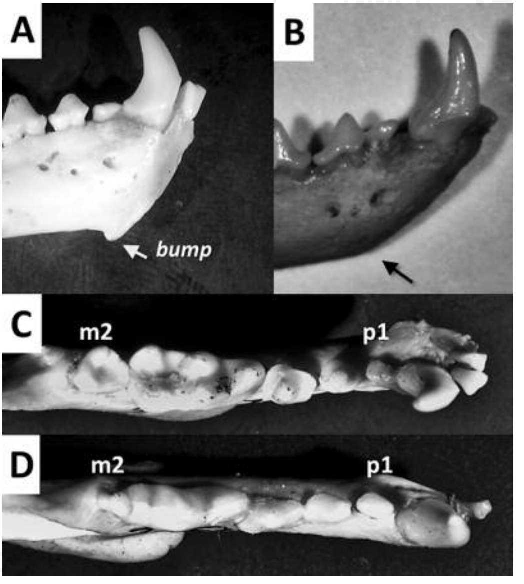

FIGURE 34. (*A. and B. labial view; C. and D. occlusal view*) Lower edge of the ramus of *Mephitis mephitis* (A) and *Mustela erminea* (B) and the size of m2 compared to p1 in *Mephitis mephitis* (C) and *Mustela erminea* (D).

45a. p2 often with a well-developed paraconid (Figure 35A); posterior edge of the vertical ramus with a distinct convex notch between the coronoid process and the condylar process (Figure 36A) . . . . *Neovison vison*
45b. p2 often without a small anterior cusp (Figure 35B); posterior edge of the vertical ramus straight between the coronoid process and the condylar process (Figure 36B) 46

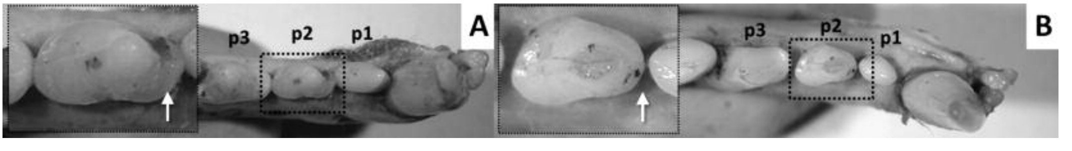

FIGURE 35. (*occlusal view*; *left: posterior*; *top: lingual*) The p2 of *Neovison vison* (A) and *Mustela frenata* (B).

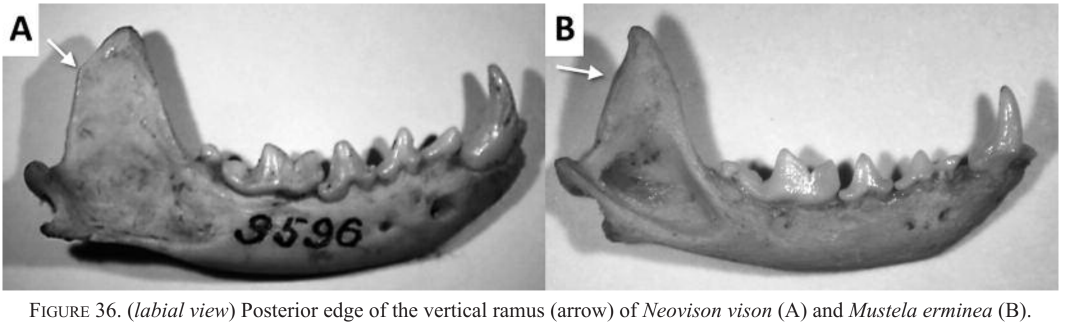

FIGURE 36. (*labial view*) Posterior edge of the vertical ramus (arrow) of *Neovison vison* (A) and *Mustela erminea* (B).

46a. Height of coronoid process <7.1 mm; length of mandibular tooth row <10 mm (Figure 37) . . . . *Mustela nivalis*
46b. Height of coronoid process >7.1 mm; length of mandibular tooth row >10 mm (Figure 37) 47

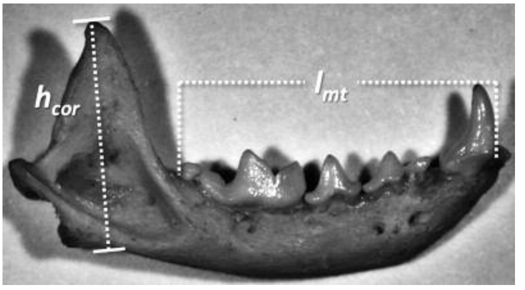

FIGURE 37. (*labial view*) Height of the coronoid process (h_{cor}) and length of the mandibular tooth row (l_{mt}) measured on *Mustela erminea*.

47a. Height of the coronoid process generally <10.5 mm; length of mandibular tooth row never >16 mm (Figure 37); posterior edge of the vertical ramus between the coronoid process and the condylar process relatively flat (Figure 38A) . . . . *Mustela erminea*
47b. Height of the coronoid process generally >10.5 mm; length of mandibular tooth row often >16 mm (Figure 37); posterior edge of the vertical ramus between the coronoid process and the condylar process with a convex curve (Figure 38B) . . . . *Mustela frenata*

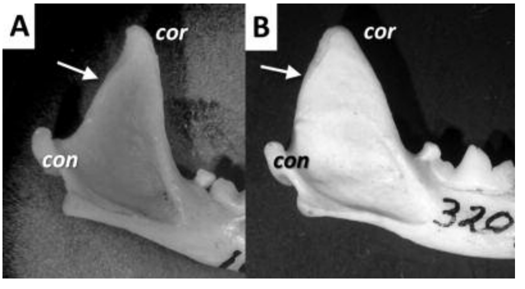

FIGURE 38. (*labial view*) Posterior edge of the vertical ramus (arrow) of *Mustela erminea* (A) and *M. frenata* (B).

48a. Presence of a clearly defined step on the lower edge of the horizontal ramus anterior to the angular process; diastemata between c1 and p1, between p1 and p2, and between p2 and p3 (Figure 39A) . . . . *Urocyon cinereoargenteus*
48b. Lower edge of the horizontal ramus anterior to the angular process smooth, without a step; only one diastema between c1 and p1 (Figure 39B) 49

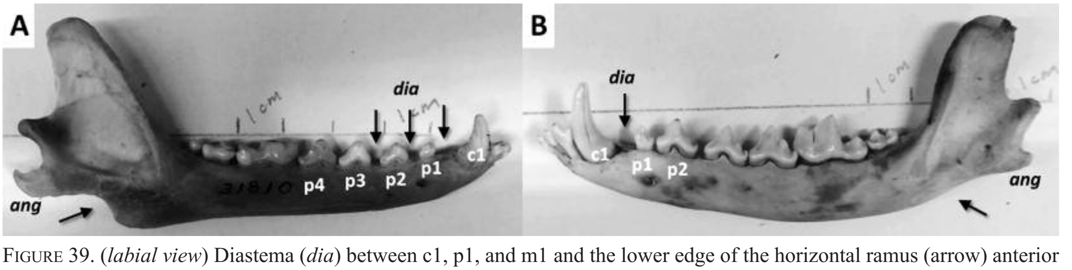

FIGURE 39. (*labial view*) Diastema (*dia*) between c1, p1, and m1 and the lower edge of the horizontal ramus (arrow) anterior to the angular process (*ang*) of *Urocyon cinereoargenteus* (A) and *Vulpes vulpes* (B).

49a. Anteroposterior length of the diastema between c1 and p1 smaller than p1 (Figure 40A) . . . *Vulpes lagopus*
49b. Anteroposterior length of the diastema between c1 and p1 about equal to p1 or larger (Figure 40B) . . . . *Vulpes vulpes*

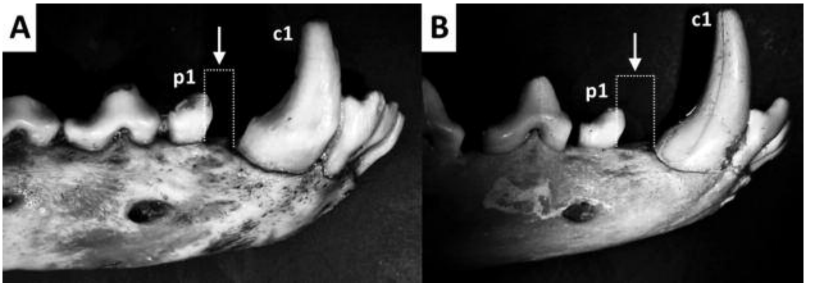

FIGURE 40. (*labial view*) Anteroposterior length of the diastema between c1 and p1 in relation to the anteroposterior length of p1 in *Vulpes lagopus* (A) and *V. vulpes* (B).

F. Chiroptera (Vespertilionidae)

50a. Three premolars (Figure 41A) 51
50b. Two premolars (Figure 41B) 54

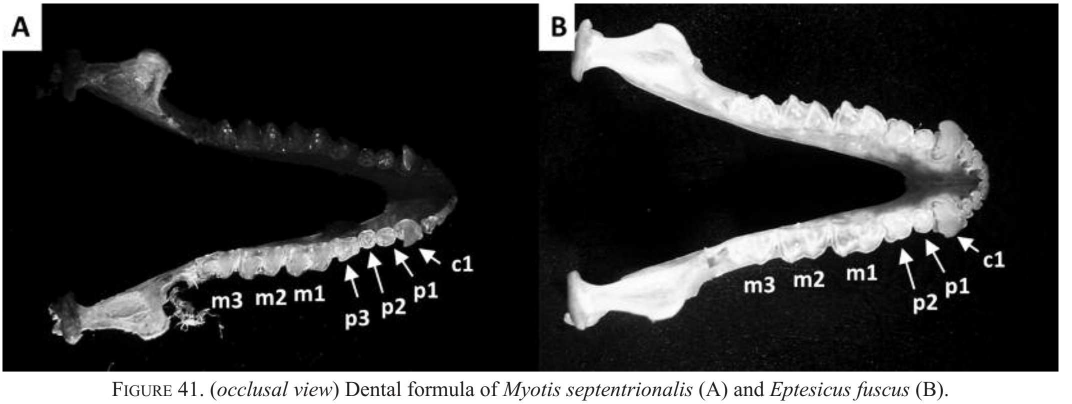

FIGURE 41. (*occlusal view*) Dental formula of *Myotis septentrionalis* (A) and *Eptesicus fuscus* (B).

51a. Mandibular length >11.5 mm (Figure 42); hypoconid of p3 with lingual crest directed medially creating a distinct lingual bulge (Figure 43A) . . . . *Lasionycteris noctivagans*
51b. Mandibular length <11.5 mm (Figure 42); hypoconid of p3 without a distinct lingual bulge (Figure 43B) 52

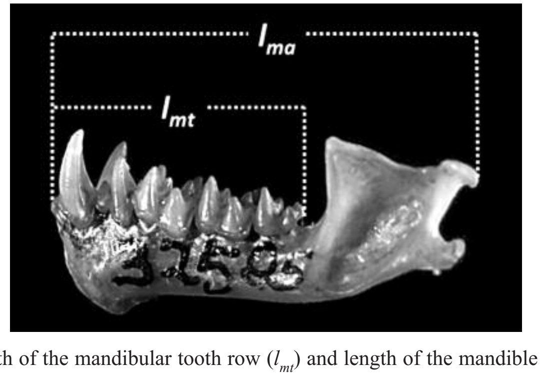

FIGURE 42. (*labial view*) Length of the mandibular tooth row (l_{mt}) and length of the mandible (l_{ma}) measured on Chiroptera (*Lasiurus cinereus*).

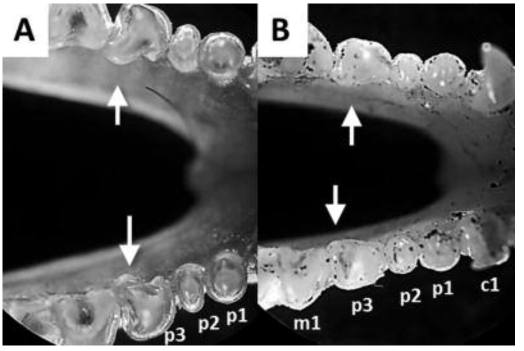

FIGURE 43. (*occlusal view*; *left: posterior*) Lingual crest of the p3 main cusp of *Lasionycteris noctivagans* (A) and *Myotis septentrionalis* (B).

52a. p3 rectangular, anteroposterior length greater than labiolingual width (Figure 44A); mandibular length generally ≥11mm (Figure 42) . . . . *Myotis septentrionalis*
52b. p3 squared, anteroposterior length approximately equal to labiolingual width (Figure 44B); mandibular length <11mm (Figure 42) 53

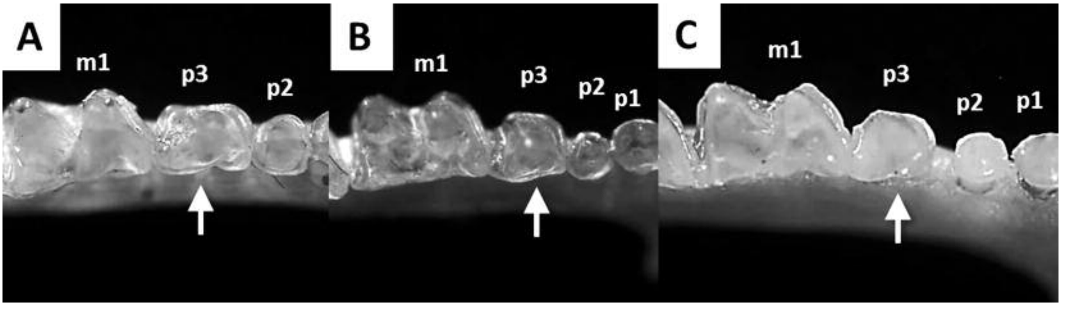

FIGURE 44. (*occlusal view*; *left: posterior*; *top: labial*) Shape of p3 in *Myotis septentrionalis* (A), *M. lucifugus* (B), and *M. leibii* (C).

53a. Mandibular length generally >10 mm; length of the mandibular tooth row generally >5.5 mm (Figure 42) . . . . *Myotis lucifugus*
53b. Mandibular length generally <10 mm; length of the mandibular tooth row generally <5.5 mm (Figure 42) . . . . *Myotis leibii*

54a. Mandibular length >12.5 mm (Figure 42) 55
54b. Mandibular length <12.5 mm (Figure 42) 56

55a. Mandibular length >14 mm (Figure 42); rounded coronoid process much taller than c1 (Figure 45A); p2 squared, with labiolingual width approximately equal to anteroposterior length (Figure 46A) . . . . *Eptesicus fuscus*
55b. Mandibular length ≤14 mm (Figure 42); sharp coronoid process approximately same height as c1 (Figure 45B); p2 rectangular with labiolingual width greater than anteroposterior length (Figure 46B) . . . . *Lasiurus cinereus*

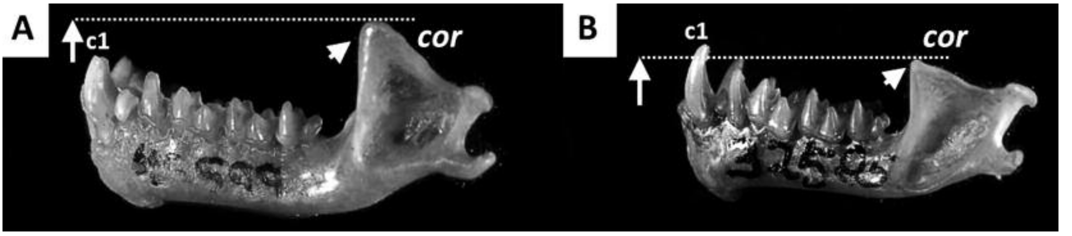

FIGURE 45. (*labial view*) Shape and height of the coronoid process (*cor*) of *Eptesicus fuscus* (A) and *Lasiurus cinereus* (B).

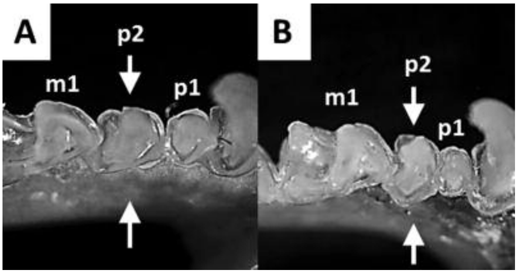

FIGURE 46. (*occlusal view*; *left: posterior*; *top: labial*) Shape of p2 of *Eptesicus fuscus* (A) and *Lasiurus cinereus* (B).

56a. Length of the mandibular tooth row <5 mm (Figure 42); small diastemata separate i2 from i3, i3 from c1, and p1 from p2; c1 approximately same height as p2 (Figure 47A) . . . . *Perimyotis subflavus*
56b. Length of the mandibular tooth row >5 mm (Figure 42); no diastema between i2 and i3, i3 and c1, or p1 and p2; c1 taller than p2 (Figure 47B) . . . . *Lasiurus borealis*

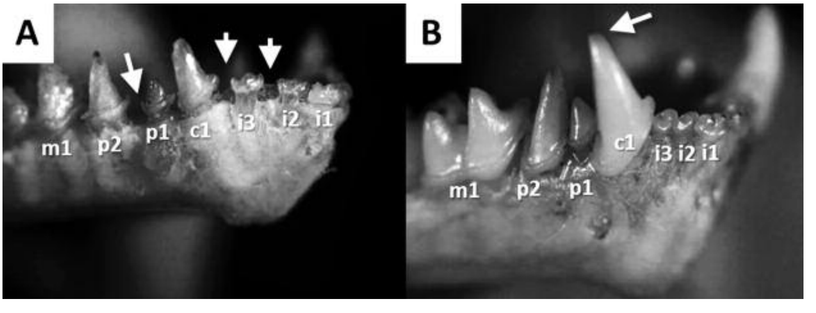

FIGURE 47. (*anterior view*) Relative size of c1 compared to p2 in *Perimyotis subflavus* (A) and *Lasiurus borealis* (B) as well as the diastemata between the incisors of *P. subflavus*.